Published in final edited form as:
Brain Struct Funct. 2010 March ; 214(2-3): 181–199. doi:10.1007/s00429-010-0244-2.

Dendritic vulnerability in neurodegenerative disease: insights from analyses of cortical pyramidal neurons in transgenic mouse models

Jennifer I. Luebke,
M949, Department of Anatomy and Neurobiology, Boston University School of Medicine, Boston, MA 02118, USA

Christina M. Weaver,
Computational Neurobiology and Imaging Center, Mount Sinai School of Medicine, New York, NY, USA, Department of Mathematics and Computer Science, Franklin and Marshall College, Lancaster, PA, USA

Anne B. Rocher,
M949, Department of Anatomy and Neurobiology, Boston University School of Medicine, Boston, MA 02118, USA

Alfredo Rodriguez,
Department of Neuroscience, Mount Sinai School of Medicine, New York, NY, USA, Computational Neurobiology and Imaging Center, Mount Sinai School of Medicine, New York, NY, USA

Johanna L. Crimins,
M949, Department of Anatomy and Neurobiology, Boston University School of Medicine, Boston, MA 02118, USA

Dara L. Dickstein,
Department of Neuroscience, Mount Sinai School of Medicine, New York, NY, USA, Computational Neurobiology and Imaging Center, Mount Sinai School of Medicine, New York, NY, USA

Susan L. Wearne, and
Computational Neurobiology and Imaging Center, Mount Sinai School of Medicine, New York, NY, USA

Patrick R. Hof
Department of Neuroscience, Mount Sinai School of Medicine, New York, NY, USA, Computational Neurobiology and Imaging Center, Mount Sinai School of Medicine, New York, NY, USA

Jennifer I. Luebke: jluebke@bu.edu

Abstract

In neurodegenerative disorders, such as Alzheimer's disease, neuronal dendrites and dendritic spines undergo significant pathological changes. Because of the determinant role of these highly dynamic structures in signaling by individual neurons and ultimately in the functionality of

Correspondence to: Jennifer I. Luebke, jluebke@bu.edu.

This review is dedicated to the memory of our beloved friend, mentor, and colleague Susan L. Wearne, who passed away in September 2009.

neuronal networks that mediate cognitive functions, a detailed understanding of these changes is of paramount importance. Mutant murine models, such as the Tg2576 APP mutant mouse and the rTg4510 tau mutant mouse have been developed to provide insight into pathogenesis involving the abnormal production and aggregation of amyloid and tau proteins, because of the key role that these proteins play in neurodegenerative disease. This review showcases the multidimensional approach taken by our collaborative group to increase understanding of pathological mechanisms in neurodegenerative disease using these mouse models. This approach includes analyses of empirical 3D morphological and electrophysiological data acquired from frontal cortical pyramidal neurons using confocal laser scanning microscopy and whole-cell patch-clamp recording techniques, combined with computational modeling methodologies. These collaborative studies are designed to shed insight on the repercussions of dystrophic changes in neocortical neurons, define the cellular phenotype of differential neuronal vulnerability in relevant models of neurodegenerative disease, and provide a basis upon which to develop meaningful therapeutic strategies aimed at preventing, reversing, or compensating for neurodegenerative changes in dementia.

Keywords

Alzheimer’s disease; Amyloid; Computational modeling; Dendritic spine; Tau; Whole-cell patch-clamp

Introduction

Neocortical pyramidal neurons possess extensive apical and basilar dendritic trees, which integrate information from thousands of excitatory and inhibitory synaptic inputs. Dendrites respond to inputs with postsynaptic potentials, which are relayed to the soma where they are summed; if a threshold potential is exceeded, an action potential is generated. Voltage attenuation in space and time along dendrites is fundamental to summation and is influenced by a number of interacting morphological properties (such as diameter and length) and active properties (such as distribution of ion channels) of the dendritic shaft (Hausser et al. 2000; Kampa et al. 2007; Stuart and Spruston 2007; Henry et al. 2008). Further complexity arises from the presence of thousands of biophysically active dendritic spines, the principal receptive site for excitatory glutamatergic inputs to a neuron.

Dendrites and dendritic spines in particular are dynamic structures, which undergo significant changes across the life span. Under non-pathological conditions, the number of spines on pyramidal neuron dendrites increases substantially over the course of development, is reduced during maturation to adulthood, and remains relatively stable during adulthood (for review see Bhatt et al. 2009). Then, during normal aging, significant changes in spine number, distribution, and morphology occur (Duan et al. 2003). Spines also undergo significant structural modifications under conditions where synaptic strength is experimentally modified, usually with protocols designed to evoke longterm potentiation or long-term depression (for review see Alvarez and Sabatini 2007; Bhatt et al. 2009; Holtmaat and Svoboda 2009). In many neurodegenerative diseases, significant alterations in the dendritic arbor occur, together with substantial spine loss and alterations in spine morphology (reviewed in Halpain et al. 2005). Gaining an understanding of these sublethal changes to neurons, which detrimentally impact neuronal signaling, and ultimately cognitive function, is an important goal.

Transgenic mouse models have been useful for elucidating mechanisms of amyloid-and tau-induced pathology, although no single model fully recapitulates human disease (for review see Duff and Suleman 2004; Spires et al. 2005). Two of the most commonly employed

mouse models of neurodegenerative disease are the Tg2576 amyloid precursor protein (APP) mutant mouse and the rTg4510 tau mutant mouse, which develop significant pathological aggregations of amyloid-beta (Aβ) and tau proteins, respectively. Tg2576 transgenic mice overexpress the Swedish double mutation of the human APP gene, which leads to progressive formation of soluble Aβ peptides and fibrillar Aβ deposits in the form of amyloid plaques. Increased Aβ levels in these mice are associated with progressive structural changes to neurons (although not with neuron death), and cognitive impairment (Hsiao et al. 1996). In the rTg4510 mouse model, expression of the P301L mutant human tau variant leads to progressive development of neurofibrillary tangles (NFTs), neuronal death, and memory impairment reminiscent of the pathology observed in human tauopathies (Santacruz et al. 2005).

In this review, we discuss changes in the structure and function of dendrites and spines of pyramidal neurons that are associated with pathological aggregation of Aβ and tau in these and other mouse models of neurodegenerative disease. We also discuss, as a point of comparison, the impact of normal brain aging on the morphofunctional properties of pyramidal neurons in aged macaque monkeys. This is not a comprehensive review of the literature on such changes in human neurodegenerative diseases or of the many studies of these changes in mouse models (for reviews see Duff and Suleman 2004; Spires and Hyman 2004; Lewis and Hutton 2005; Duyckaerts et al. 2008; Giannakopoulos et al. 2009). Rather, the focus here is specifically on our multidimensional collaborative efforts to understand the functional consequences of pathological changes in the structure of individual layer 3 frontal cortical pyramidal neurons in commonly employed mouse models of neurodegeneration. These studies focus on layer 3 pyramidal neurons in the neocortex because they are the principal neurons involved in corticocortical circuits that mediate many cognitive functions of the frontal cortex and may be selectively targeted in neurodegenerative disease (Morrison and Hof 1997, 2002; Hof and Morrison 2004). Following a brief overview of the normal structure and function of dendrites and spines, we describe technical details of our experimental approach and the analytical tools we have developed to reconstruct and quantify dendritic and spine structure in 3D in mouse and macaque monkey models (Rodriguez et al. 2003, 2006, 2008, 2009; Wearne et al. 2005; Rocher et al. 2008, 2009; Kabaso et al. 2009). Next, empirical structural and electrophysiological data obtained from frontal cortical pyramidal neurons in in vitro slices prepared from transgenic versus wild-type mice are discussed. Finally, we end with a description of the computational modeling approaches currently used by our group to provide insights on structure–function relationships in pyramidal neurons under pathological conditions mimicking those seen in human neurodegenerative diseases (Rothnie et al. 2006; Henry et al. 2008; Weaver and Wearne 2008; Kabaso et al. 2009).

Normal structure and function of dendrites and spines

Dendrites

The architecture of dendritic arbors varies extensively, from the relatively simple arbors of anterior horn neurons in the spinal cord, to the more complex cortical pyramidal neurons, to the extreme elaboration seen in cerebellar Purkinje neurons. Despite the large variability in the numbers of dendritic branches and their overall extent, most dendrites share certain fundamental characteristics, including that they are wide at the base and taper as they extend distally, and they branch at angles <90°. The organelles in dendrites are similar to those found in the soma; rough and smooth endoplasmic reticulum, free ribosomes, mitochondria, neurofilaments, and microtubules are all present, abundantly in the wide proximal bases, and decreasingly as dendrites move distally and decrease in diameter. As shown in Fig. 1a, layer 3 cortical pyramidal neurons have a skirt of basilar dendrites originating from the base and a main apical dendrite originating from the apex of their soma. The main apical dendrite gives

rise to several oblique branches and, approximately at the intersection between layers 2 and 1, to an apical tuft that ascends to the pial surface. Importantly, the basilar and apical dendritic domains receive and integrate inputs from anatomically and functionally distinct presynaptic sources (for review see Spruston 2008). Basilar and proximal apical dendrites receive inputs from layer 4 neurons and from local-circuit neurons (Lubke et al. 2000;Feldmeyer et al. 2002). The apical tuft, which can comprise up to 50% of the dendritic arbor of a given neuron, is the principal recipient of monoaminergic modulatory inputs (Thierry et al. 1990), thalamic inputs (van Groen et al. 1999), and feedback intracortical connections (Rockland and Pandya 1979).

The structural properties of dendrites underlie their passive membrane (cable) properties, which are membrane capacitance C_m, specific membrane resistance R_m and axial resistivity R_a. These cable properties determine, at a fundamental level, the degree of summation of synaptic inputs and the spatial distribution of electrical signals. Because summation of synaptic inputs by dendrites is determined in large part by their structure, dendritic morphology plays a critical role in action potential generation (Mainen and Sejnowski 1996; Koch and Segev 2000; Euler and Denk 2001; Vetter et al. 2001; Krichmar et al. 2002; Ascoli 2003). Importantly, both branching topology and surface irregularities including dendritic varicosities (Surkis et al. 1998) contribute to the excitable properties of neurons. For example, recent simulation studies have demonstrated that marked differences in the efficacy of action potential back propagation in different neural types are attributable in large part to variations in dendritic morphology (for review see Stuart et al. 1997; Waters et al. 2005).

Integration of synaptic inputs by dendrites is mediated not only by basic passive cable properties, but also by active properties, which include the number and distribution of voltage, ligand, as well as second messenger-gated transmembrane ionic channels (reviewed in Migliore and Shepherd 2002; Magee and Johnston 2005; Johnston and Narayanan 2008; Nusser 2009). Dendrites possess a rich array of sodium, calcium, and potassium channels that are distributed either uniformly or non-uniformly across a given dendrite (for reviews, see Johnston et al. 1996; Migliore and Shepherd 2002; Magee and Johnston 2005; Johnston and Narayanan 2008; Nusser 2009). For example, layer 5 cortical pyramidal neuron dendrites possess a gradient of the hyperpolarization-activated mixed cationic HCN channels that increase in density from the soma to the apical tuft (Berger et al. 2001; Lorincz et al. 2002). The interaction of intrinsic ionic and synaptic conductances with passive properties determined by dendritic morphology can effectively alter the cable properties of the dendritic tree (Bernander et al. 1991; Segev and London 2000; Bekkers and Hausser 2007) adding a further layer of complexity to signaling by individual neurons. Computational modeling approaches have been extensively employed to shed light on dendritic structure–function relationships and into potential interactions between a multitude of dendritic active and passive properties. These approaches, as discussed at the end of this review, have been useful for gaining insight on dendrites that are too thin to be studied with electrophysiological approaches, and for providing empirical researchers with testable hypotheses relevant to the functional consequences of dendritic dystrophy in neurodegenerative diseases.

Dendritic spines

Dendrites of glutamatergic pyramidal neurons are studded by thousands of dendritic spines, which are the site of most of the glutamatergic synapses in the brain, that confer further functional complexity to these processes. Spine density, shape, and distribution are all important contributors to neuronal excitability that are superimposed on the electrophysiological properties of dendritic shafts (Wilson 1988; Stratford et al. 1989; Baer and Rinzel 1991; Tsay and Yuste 2002). Spines are small appendages that extend from

approximately 0.5–3 lm from dendritic shafts and are usually <1 μm in diameter (Fig. 1b, c). Mouse layer 3 frontal cortical pyramidal neurons typically possess approximately 6,000 dendritic spines (Rocher et al. 2008). Spines can be broadly categorized as falling into one of several different morphological types, namely “thin”, “stubby”, “mushroom”, and “filopodia” which are normally seen in large numbers only during development (for review see Yuste and Bonhoeffer 2004; Bourne and Harris 2007). Although most spines do fall into one of these broad categories, serial electron microscopy reveals that there is also a continuum between the different morphological subtypes (Bourne and Harris 2007). Spine morphology determines the strength, stability and function of excitatory synaptic connections that subserve the neuronal networks underlying cognitive function. Smaller spines, such as the thin and filopodia types are less stable and more motile (Trachtenberg et al. 2002; Kasai et al. 2003; Holtmaat et al. 2005) and as a result, are more plastic than large spines such as the mushroom and stubby types (Grutzendler et al. 2002). The size and morphology of the spine head is correlated with the number of docked presynaptic vesicles (Schikorski and Stevens 1999) and the number of postsynaptic receptors (Nusser et al. 1998), and hence with the size of synaptic currents and synapse strength. In addition, a small head size permits fast diffusion of calcium within the spine, while the neck length shapes the time constant for calcium compartmentalization (for review see Yuste and Bonhoeffer 2001; Nimchinsky et al. 2002), modulating postsynaptic mechanisms that play an important role in synaptic plasticity linked to functions, such as learning and memory (Holthoff et al. 2002; Alvarez and Sabatini 2007; Bloodgood and Sabatini 2007). Spine neck length and diameter also affect diffusional coupling between dendrite and spine (Svoboda et al. 1996; Yuste et al. 2000; Bloodgood and Sabatini 2005), and spine density and shape regulate the degree of anomalous diffusion of chemical signals within the dendrite (Santamaria et al. 2006). Spine morphology also varies dynamically in response to synaptic activity (Lendvai et al. 2000; Hering and Sheng 2001; Zuo et al. 2005).

Over the past few decades, it has become increasingly evident that local dendritic spine structure and distribution (Matus and Shepherd 2000) play a key role in the electrical and biochemical signaling of dendrites (Nimchinsky et al. 2002; Matus 2005; Bourne and Harris 2007). However, spines present challenges to the standard cable model of dendrites. The common way to model the effects of spines in a passive cable equation model is to reduce the membrane resistance and increase the membrane capacitance by a factor proportional to the increased membrane surface area due to spines (Jaslove 1992). This modification predicts that voltage should attenuate more drastically in space along spiny dendrites, relative to their smooth counterparts. Because of their capacity for plasticity and because they are the location of most excitatory synapses in the cerebral cortex, accurately characterizing the structure of dendritic spines is essential for understanding their contributions to neuronal, and ultimately to cognitive function.

Current methods used to study the structure of dendrites and spines

Experimental approaches

The most widely employed method used to study the dendritic structure of neurons has historically been the Golgi impregnation method, in which neurons are impregnated by silver chromate following incubation in potassium dichromate and silver nitrate. This method was developed by Camillo Golgi and used by Ramón y Cajal in his seminal descriptions of neurons at the turn of the twentieth century (Ramón y Cajal 1911; Garcia-Lopez et al. 2007). The Golgi method has been used in innumerable studies designed to examine the normal structure of neurons, as well as changes in neuronal structure across the lifespan or under pathological conditions. This approach has been used in a number of studies designed to examine the effects of Alzheimer’s disease (AD) on neuronal structure (Paula-Barbosa et al. 1980; Probst et al. 1983; Ferrer et al. 1990; Flood 1991; Gertz et al.

1991; Scott 1993; Garcia-Marin et al. 2007). However, the Golgi technique has a number of significant drawbacks that make it suboptimal for high-resolution analyses of neuronal structure. First, it is capricious; neurons are stained in a random and unpredictable manner. Second, axons and distal dendritic processes are often incompletely impregnated, and given that dendritic retraction and extension is a common feature of pathological states, this is a significant methodological drawback. Third, as neurons are not fluorescently labeled, they cannot be analyzed at very high resolution in 3D with confocal laser scanning microscopy (CLSM) or with multiphoton laser scanning microscopy (MPLSM).

Improved techniques using fluorescence labeling to assess the details of dendrite and dendritic spine structure are now available. These techniques are ideally suited for imaging neurons at a very high resolution with CLSM/MPLSM for subsequent 3D reconstruction. In lightly fixed tissue, neurons can be well filled by intracellular injection of fluorescent dyes, such as Lucifer Yellow (Rho and Sidman 1986; Buhl and Lübke 1989). In living tissue, DiOlistic labeling using the ballistic delivery of lipophilic dye-coated particles (Moolman et al. 2004; Tsai et al. 2004) and GFP labeling with the gene transfer technique by viral vectors (Spires et al. 2005) have been used in the examination of changes in the structural properties of neurons in transgenic mouse models of AD. In these studies, transcranial two-photon laser scanning microscopy of fluorescently labeled neurons was used to great advantage in the study of dendritic and spine changes in vivo, as a consequence of proximity to amyloid plaques in cortical pyramidal neurons in Tg2576 APP mutant mice (e.g., Tsai et al. 2004; Spires et al. 2005). Injection of biocytin during electrophysiological recordings and subsequent incubation of the tissue with fluorescent avidin compounds is a useful means by which both the function and structure of individual neurons can be characterized. We have used this approach to examine structure–function relationships in neurons from mouse models of neurodegenerative disease (Rocher et al. 2008, 2009) and from normally aging macaque monkeys. Biocytin filling during recordings yields exquisitely labeled dendrites, spines and axons (Figs. 1, 2, 3, 4, 5), and allows for the correlation of high-resolution morphometric data with detailed electrophysiological data, providing important information on structure–function relationships.

3D reconstruction and analytical approaches

Early methods for digitizing 3D neuronal structures relied on interactive manual tracing from a computer screen (Capowski 1985). These methods were time-consuming, subjective, and lacked precision. In recent years, automated methods have been developed that use image analysis algorithms to extract neuronal morphology directly from 3D microscopy and overcome the limitations of manual techniques (Koh et al. 2002; He et al. 2003; Wearne et al. 2005). Newer methods use pattern recognition routines to track or detect a structure locally without the need for global image operations (Al-Kofahi et al. 2002; Streekstra and van Pelt 2002; Schmitt et al. 2004; Myatt et al. 2006; Santamaria-Pang et al. 2007). Most are designed to work on a broad range of signal-to-noise ratios and even on multiple imaging modalities. This results in increased computational complexity, which makes the use of these methods as interactive reconstruction tools for high-resolution data less than optimal.

In our studies of neuronal structure, morphological reconstruction is performed using NeuronStudio, a neuron morphology reconstruction software tool (http://www.mssm.edu/cnic/tools.html), developed by Wearne et al. (2005) and Rodriguez et al. (2006, 2008, 2009). Neuron- Studio has been designed for low computational complexity to allow interactive semi-automated extraction of neuronal morphology from medium to high-quality de-convolved 3D CLSM and MPLSM image stacks of fluorescently labeled neurons. It features automated extraction of dendrites and dendritic spines as well as a rich set of manual editing and visualization modalities. Figure 2a shows an *xy* projection of CLSM data from a wild-type mouse layer 3 cortical pyramidal neuron and Fig. 2b shows the

automated reconstruction of the neuron's dendritic arbor obtained using NeuronStudio. Because fluorescence intensity can vary with adequacy of filling, imaging depth and *xy* spatial extent in CLSM and MPLSM image stacks, data segmentation within NeuronStudio adapts the iterative self-organizing data analysis (ISODATA) method (Ridler and Calvard 1978) to compute local thresholds dynamically. This method is appropriate for datasets exhibiting a bimodal distribution of intensity values, such as the grayscale images characteristic of de-convolved LSM image stacks.

Automated 3D reconstruction of dendritic arbors

To reconstruct the dendritic arbors automatically from an image, we first look to extract the 'centerline' of each dendritic segment: the line that identifies the center of the dendrite as it traverses through space (blue line in Fig. 2c). In NeuronStudio, dendritic centerline extraction is performed using the voxel scooping method (Rodriguez et al. 2009). Voxel scooping is an efficient algorithm for centerline extraction from volumetric datasets of fluorescently labeled neurons obtained by CLSM imaging. Starting from a seed location inside the structure, the method iteratively carves thin cross sectional layers of object voxels ('scoops') that are clustered based on the connectivity. Each cluster contributes a node along the centerline, which is created by connecting successive nodes until all object voxels are exhausted. The actual position where each node is created depends on a number of cluster parameters to ensure proper centering along the dendrite. The addition of voxels to each cluster is also done in a way that allows the algorithm to advance into the structure while adjusting for directional changes. The scooping method provides an optimal balance between computational efficiency and tracing accuracy that is suitable for interactive neuron tracing applications. The resulting model is amenable to manual editing and is compatible with compartment modeling packages such as NEURON (Carnevale and Hines 2006) and GENESIS (Bower and Beeman 1998), and with morphometry analysis software such as L-Measure (Scorcioni and Ascoli 2001).

Diameter estimation in NeuronStudio is performed using the Rayburst sampling algorithm (Rodriguez et al. 2006) to determine the minimum wall-to-wall span at each node location inside the dendrite or spine (Fig. 2d). For data acquired by LSM, the point-spread function of the microscope can distort the apparent thickness of branches significantly along the direction of the optic axis (usually the *z* axis of the data). Although this is largely reduced by deconvolution, residual smear along the optic axis is not uncommon. The 2D variant of the Rayburst algorithm is insensitive to residual smear along the optic axis, and can produce a reliable estimate of branch diameter regardless of the orientation of the branch within the image stack when run centrally within a branch of approximately circular cross section.

Automated 3D reconstruction of dendritic spines

The assessment of spine numbers and distribution and their classification into subtypes has historically been a labor intensive and relatively inaccurate process. Spine numbers could only be estimated because spines extending primarily in the *z* plane relative to the dendritic shaft could not be counted. With the advent of CLSM, accurate 3D spine assessment came a step closer, but was still a highly timeconsuming and labor-intensive undertaking. Improving upon previous spine detection algorithms (Koh et al. 2002; Cheng et al. 2007), Rodriguez et al. (2008) devised an efficient and robust method for automated spine detection, available in NeuronStudio. To detect spines, NeuronStudio begins by building concentric layers of voxels around a previously computed model of the dendritic structure. Voxels are segmented by interpolating ISODATA thresholds computed at each node along the dendritic model. The algorithm only processes object voxels within a maximum user-specified distance from the model and makes use of space partitioning to achieve faster processing. Individual spines are detected by clustering voxels in layers starting from the most distal voxels. For

each processed object voxel, the algorithm computes the distance to the model's surface (DTS). Any voxel having no neighbor with a greater DTS is considered a local maximum or tip and is evaluated as a possible spine. Using this maximum as a first layer, each iteration of the algorithm builds a new layer by first adding unvisited voxels directly connected to the previous layer and then expanding the new layer with any connected voxels having a DTS value equal or greater than the lowest DTS in the layer. This results in the formation of thin concentric layers that are used to measure the shape of a protrusion and to determine if a spine has been found. The algorithm also measures the Rayburst diameter at the center of each layer to build a measurement profile that is used to further characterize the spine shape into thin, stubby, or mushroom morphologic types. An example of spines characterized by NeuronStudio's spine detection algorithms is shown in Fig. 2d.

3D measures of spatial complexity

Traditionally, Sholl analysis (1953) has been used in two dimensions to quantify the spatial complexity of dendritic branching patterns with increasing distance from the soma. Fractal analyses have also been used (Smith et al. 1989; Caserta et al. 1995; Jelinek and Elston 2001; Henry et al. 2002) to quantify spatial complexity as a power law scaling exponent, describing the rate of change of the number of branches over a large portion of the dendrites, and best visualized as the slope of a log–log plot of these two quantities. We have recently extended this work (Rothnie et al. 2006; Kabaso et al. 2009) to include three power law exponents describing global spatial complexity: rates of change of dendritic mass, branching, and taper.

We analyzed these power law exponents (log–log slopes) in two types of layer 3 pyramidal neurons of rhesus monkeys: those located in the superior temporal cortex with 'long' corticocortical projections to area 46, and those with 'local' projections within area 46. We studied apical and basal dendrites separately, and compared results in young and old rhesus monkeys (Duan et al. 2003; Kabaso et al. 2009). Consistently in each of these neurons, we found that the rate of change of dendritic mass was constant in two distinct regions of the dendrites (Rothnie et al. 2006; Kabaso et al. 2009). These regions (region I: 'proximal' and region II: 'medial') and associated scaling exponents are shown in Fig. 2e for the apical dendrites of a typical long projection neuron from a young monkey. The mean and standard errors of scaling exponents for all young long projection neurons are shown in Fig. 2f.

Rothnie et al. (2006) revealed a form of global mass homeostasis in these neurons: the rates of branching and tapering in each of the two regions were inversely related, so that the spatial gradient of dendritic mass with distance from the soma was constant. Significantly, we found that the compensation of branching and tapering was maintained across the different projection types, and even with aging, so that the spatial gradient of dendritic mass in the proximal and medial regions was constant (Kabaso et al. 2009). This global mass homeostasis might be due to some kind of control mechanism intrinsic to the neuron (Samsonovich and Ascoli 2006) that is conserved in aging. It will be instructive to evaluate whether such global mass homeostasis is maintained during neurodegeneration.

In conclusion, these analytical tools provide rapid, objective analyses of the high-resolution data that we collect from wild-type and transgenic mouse neurons. With NeuronStudio, we are able to perform analyses of differences in dendrite diameter and spine shapes that were not available previously, and these kinds of studies are currently ongoing in our laboratories. Moving forward, we will evaluate whether the global patterns in spatial complexity observed in rhesus monkey pyramidal neurons are similarly present in mouse neurons. We will also compare the spatial complexity of wild-type and transgenic neurons to determine whether global mass homeostasis is conserved in neurodegeneration as it seems to be in aging.

Alterations in the structure of dendrites and spines of cortical pyramidal neurons in Tg2576 and rTg4510 mutant mice

Dendritic changes in neurodegenerative disease

Numerous studies have demonstrated pervasive and significant changes in neuronal morphology in AD and other neurodegenerative diseases (Anderton et al. 1998; Falke et al. 2003; Knobloch and Mansuy 2008; Giannakopoulos et al. 2009; Tackenberg et al. 2009). Proximity to fibrillar Aβ plaques, both in AD and in mouse models which overexpress APP, has been positively associated with dystrophic dendrites and axons, aberrant sprouting and curvature of dendritic processes and loss of dendritic spines with accompanying synapse loss in hippocampal and neocortical pyramidal cells (Knowles et al. 1999; Le et al. 2001; Urbanc et al. 2002; Tsai et al. 2004; Spires et al. 2005; for review Spires and Hyman 2004). For example, Tsai et al. (2004) showed prevalent axonal varicosities and reduced diameter of dendrites directly traversing or closely apposed to fibrillar Aβ plaques in PSAPP transgenic mice and Spires et al. (2005) reported significantly altered trajectories of dendrites from neocortical pyramidal neurons near Aβ plaques in Tg2576 mice.

The effects of soluble Aβ on dendritic structure are less well characterized. Using the dendritic and spine reconstruction and analysis methods provided in NeuronStudio, we examined the morphological and electrophysiological properties of layer 3 frontal cortical pyramidal neurons in brain slices from 12-month-old Tg2576 mice (an age at which soluble Aβ levels are high but there are few Aβ plaques). Whole-cell patch-clamp recording with simultaneous biocytin filling of neurons was used for a detailed and comprehensive assessment of the dendritic morphology of entire neurons (Fig. 3a). Dendritic properties of pyramidal neurons from 12-month-old Tg2576 mice were notably altered from those from wild-type mice, exhibiting significantly increased spatial extents, lengths, and volumes across the full expanse of both apical and basal dendritic arbors (Rocher et al. 2008).

In another study, we examined morphological changes in the Tg2576 mouse frontal pyramidal neurons at 9 and 24 months of age, using cell filling with Lucifer Yellow in lightly fixed tissue (Dickstein et al. unpublished data). There was no difference in dendritic structure between the Tg2576 and wild-type neurons at 9 months of age, prior to substantial deposition of plaques. However at 24 months of age, when amyloid plaques are abundant, we observed a significant reduction in apical dendritic length when compared with wild type in layer 3 pyramidal neurons (~ 22% decrease). Taken together, data from these studies indicate that dendritic structure is modified with time in Tg2576 cortical pyramidal neurons, with an initial elongation at 12 months followed by regression at 24 months.

In contrast to studies on the effects of Aβ on dendritic morphology, very little is known about the effects of mutated tau on neuronal structure. Under normal conditions, the microtubule-associated protein tau plays a key role in stabilization and assembly of microtubules, which are critical for the maintenance of normal cellular morphology and cellular trafficking (Conde and Caceres 2009). In neurodegenerative diseases, such as AD and animal models of tauopathy, mutated and/or overexpressed tau becomes hyperphosphorylated, disengaged from microtubules and relocalized from the axon to the somata and dendrites where it aggregates in the form of NFTs and neuropil threads, respectively (Spires-Jones et al. 2009). The overexpression of tau, like that which occurs in rTg4510 mice, has been shown to result in destabilization of the dendritic cytoskeleton and compromised intracellular trafficking (Hall et al. 2000, 2001). Although there is a strong positive relationship between the number of NFTs and the severity of neurodegeneration and dementia in AD, recent studies question whether NFTs are themselves toxic to neurons. There is an apparent dissociation between the presence of an NFT and neuron death as

demonstrated by Andorfer et al. (2005) who found that in htau mice (which overexpress wild-type human tau), substantial neuronal death precedes NFT formation, and dying neurons lack evidence of fibrillar tau aggregates. In a recent study, we assessed the effect of overexpression of mutant tau on neuronal structure and function in rTg4510 mice at 8.5 months of age (Rocher et al. 2009). Forty-two percent of the rTg4510 neurons assessed in this study contained a thioflavin S-positive NFT in the somata, and the remaining 58% did not stain with thioflavin S (Fig. 3b). The majority of rTg4510 neurons (65%) exhibited marked atrophy or complete loss of the apical dendritic tuft. This morphological remodeling occurred regardless of the presence or the absence of NFTs. Further, both apical and basal dendrites of rTg4510 neurons demonstrated significantly diminished length and complexity. Recently, Dickstein et al. (this issue) compared the dendritic structure of cortical pyramidal neurons from htau mice at 3 months of age, when hyperphosphorylated tau is present, but NFTs are not, to neurons at 12 months of age when NFTs are evident. There were no significant differences in apical or basal dendritic length between neurons from the two age groups; however, neurons from 12-month-old mice had significantly more complex proximal apical dendrite branching patterns as compared to neurons from younger mice (~ 15% increase in density in the segments 30–120 lm from the soma). Future studies will compare neurons from htau mice versus those from wild-type controls and also examine alterations to dendritic structure in htau mice at older ages when tauopathy is more established.

Spine changes in neurodegenerative disease

Many studies have shown that dendritic spines are particularly vulnerable in AD and in mouse models of AD (for review see Knobloch and Mansuy 2008; Giannakopoulos et al. 2009). Loss of approximately half of dendritic spines has been reported for cortical pyramidal neuron dendrites directly traversing or closely apposed to Ab plaques in aged PSAPP (46%; Tsai et al. 2004) and Tg2576 mice (50%; Spires et al. 2005). Although the majority of studies have concentrated principally on morphological alterations of neurons associated with fibrillar plaques, comparable changes have been observed in areas devoid of Aβ deposits. In neurons from PSAPP mice, spine loss has been reported in regions with minimal or no fibrillar Aβ (Tsai et al. 2004), and in Tg2576 mice there is a substantial ~ 25% loss of spines on dendrites not in close proximity to Aβ plaques (Spires et al. 2005).

To determine the effect of endogenous soluble Aβ species on neuronal morphology in young Tg2576 mice prior to substantial plaque deposition, we assessed the number, density, and distribution of spines across the entire apical and basal dendritic arbors of layer 3 frontal cortical pyramidal neurons from Tg2576 versus wild-type mice at 12 months of age (Rocher et al. 2008). Spines were evaluated in 3D using high-resolution confocal imaging followed by automated spine detection with NeuronStudio. Although the distribution and mean total number of dendritic spines did not differ between the two groups, neurons from Tg2576 mice exhibited a significantly decreased mean density of spines per unit dendritic volume in both the apical and basal trees (Fig. 4). Comparable to reductions reported by others for individual dendritic segments (Tsai et al. 2004; Spires et al. 2005), spine density was significantly decreased (−26%) across the entire dendritic arbor in Tg2576 neurons. There was a strong relationship between spine number and total neuron volume in individual neurons, indicating that the total number of spines is preserved in Tg2576 neurons as a result of concomitant dendritic lengthening. During the early stage of disease progression prior to substantial plaque formation, but at which time, soluble Aβ species are abundant, it is plausible that the total number of dendritic spines ismaintained through compensatory dendritic elongation. At later stages, the formation of plaques is accompanied by abnormal neurite curvature and continued spine loss. It is at this time,when the Aβ load is much higher, that progressive alterations in neuronal morphology will likely lead to significant

functional consequences such as altered synaptic integration as observed in vivo in mice with fibrillar Aβ plaques (Stern et al. 2004).

In a recent study on pyramidal neurons from 9-monthold versus 24-month-old Tg2576 mice (Dickstein et al. unpublished data), there was a shift in the proportion of morphological subtypes of spines, with a significant reduction in number of mushroom and stubby spines and an increase in the number of thin spines. This shift in spine type was accompanied by a change in specific spine volumes with thin spines of neurons from 24-month-old mice having significantly larger volumes than those from 9-month-old mice. Larger thin spines may represent a regression of mushroom spines suggesting a loss of stable, mature spines in neurons from 24-month-old Tg2576 mice.

There is not much information available about the effects of tauopathy on dendritic spines of cortical pyramidal neurons. Evidence that spine numbers are reduced comes from studies showing a ~ 40% decrease in the density of synaptophysin labeling in the prefrontal cortex (PFC) of patients with frontotemporal dementia (Liu et al. 1996) and studies of synaptic markers in transgenic mouse models of tauopathy. There is a reduction in spinophilin and synaptophysin labeling and spine–synapse density in the hippocampus of the ΔK280 proaggregation model of tauopathy (Mocanu et al. 2008), and a similar reduction in synaptotagmin and synaptophysin immunoreactivity in the hippocampus of the THY-Tau22 mouse model (Schindowski et al. 2006). We recently demonstrated that, in addition to dramatically altering the dendritic shafts of cortical pyramidal neurons, mutated tau expression leads to a significant ~ 30% reduction in dendritic spine density on pyramidal neurons from rTg4510 mice (Fig. 4; Rocher et al. 2009). Further, in neurons from htau mice, there were significant differences in apical spine density in cells from mice at 3 versus 12 months of age with no differences in basal dendrites (Dickstein et al. this issue). The changes in spine number were accompanied by a significant decrease (~ 44%) in overall spine volume in dendrites of neurons from 6 and 12-month-old htau mice. Interestingly, as with spines in the aged Tg2576 mice, there was a shift from stable mushroom spines to thin spines with an increase (~ 17%) in the volume of thin spines, indicating that comparable mechanisms of spine destabilization may occur in these two mouse models.

In summary, significant structural changes are induced in dendrites and spines by aberrant tau and amyloid, which could be expected to have significant functional consequences. Importantly, there is growing evidence that these morphological changes are reversible, at least in mouse models of neurodegenerative disease. For example, recent studies have demonstrated reversal of dendritic pathology in APP/PS1 mutant mice upon treatment with both rolipram and TAT-HA-Uch-L1 (Smith et al. 2009) or with Aβ immunotherapy in Tg2576 and APP/PS1 mice (Lombardo et al. 2003; Biscaro et al. 2009; Rozkalne et al. 2009).

Functional consequences of neurodegenerative morphological changes

Insights from electrophysiological studies

As summarized above, the structural characteristics of individual neurons fundamentally determine their functionality with respect to both synaptic integration and firing properties. Therefore, it is likely that the altered morphology of Tg2576 and rTg4510 pyramidal neurons result in modifications of functional electrophysiological properties of individual neurons and downstream neuronal network properties. However, there is a dearth of information on the functional consequences of significant morphological changes in APP and tau transgenic mice. Some insight has been provided by studies in which soluble Aβ protofibrils exogenously applied to isolated embryonic rat neocortical neurons elicited a marked increase in neuronal excitability (Hartley et al. 1999) and inhibition of A and D type

outward potassium currents (Ye et al. 2003). Several studies have demonstrated that basal glutamatergic synaptic transmission (assessed with extracellular field potential recordings) is significantly reduced in populations of cells in the hippocampus and neocortex of APP transgenic mice as compared to control mice (Larson et al. 1999; Hsia et al. 1999; Giacchino et al. 2000; Fitzjohn et al. 2001; Roder et al. 2003; Brown et al. 2005). In addition, a significant reduction in LTP in the hippocampus of Tg2576 mice has been reported (Chapman et al. 1999; Kamenetz et al. 2003; Wang et al. 2004) and intracerebroventricular injection of soluble Aβ protein inhibits hippocampal LTP in vivo, providing evidence for a role for soluble Aβ in this effect (Walsh et al. 2002; Klyubin et al. 2004). Finally, a recent in vivo study using a genetically encoded calcium indicator to assess neuronal calcium levels in spines and dendrites showed disrupted calcium homeostasis and dystrophic neurites in close proximity to amyloid plaques in APP/PS1 mutant mice (Kuchibhotla et al. 2008).

In our electrophysiological studies of layer 3 frontal cortical pyramidal neurons, we found no significant difference in passive membrane or action potential firing properties between Tg2576 neurons and wild-type neurons (Rocher et al. 2008; Fig. 5a). Importantly, despite a significant reduction in dendritic spine density, the frequency, amplitude, and kinetics of spontaneous excitatory synaptic currents in the same neurons also remained unchanged. This preservation of glutamatergic signaling was likely due to the maintenance of spine numbers, despite reductions in spine density due to elongation of dendritic processes. It remains to be seen whether there are more marked functional consequences of the more dramatic structural alterations seen in pyramidal neurons from older Tg2576 mice.

In a recent study on layer 3 cortical pyramidal neurons from 8.5-month-old rTg4510 mice (Rocher et al. 2009), we observed major alterations in dendritic architecture (loss of the apical tuft), and spine density changes that could lead to substantial modification of functional electrophysiological properties, particularly with regard to integration of synaptic inputs. Direct measurement of electrophysiological properties in these cells with whole-cell patch-clamp recordings revealed that input resistance and membrane time constant were comparable between rTg4510 and wildtype neurons. These findings are expected as both properties are related to soma and total neuron surface area, which were similar between both groups. Importantly, resting membrane potential was significantly depolarized in rTg4510 neurons. This is possibly due to the significantly increased depolarizing “sag” potential also observed in rTg4510 neurons, disturbances in ATPase pump function linked to mitochondrial dysfunction, and/or decreased inhibitory synaptic inputs. In addition, rTg4510 neurons exhibited increased action potential firing frequency, reflecting the reduction in depolarization required to elicit action potentials (Fig. 5b). The implications of this excitability increase for the activity of individual neurons and networks of neurons are significant, and could be viewed as both potentially detrimental and beneficial. Increased excitability could be detrimental in that the dynamic range for the modulation of the rTg4510 neurons would necessarily be reduced due to a “ceiling effect” in which they are closer tomaximal firing rates than are wild-type neurons when depolarized from rest. On the other hand, increased excitability may favor maintenance of more normal network behavior in the face of significantly reduced glutamatergic synaptic transmission within a network.

Clearly, there is a need for many more studies on the functional electrophysiological consequences to individual neurons of the significant structural changes in neurodegenerative disease. Given the lack of such studies, and also technical considerations such as space clamp limitations and the impossibility of recording from distal dendrites or spines, the use of modeling methods to understand potential functional consequences of structural changes is very important.

Insights from modeling

For nearly 60 years, mathematical models have been used to investigate neuronal function. Hodgkin and Huxley's (1952) mathematical model of action potential generation predicted the existence of ion channels, decades before ion channels were observed experimentally (Neher and Sakmann 1976). Other models were groundbreaking in describing how dendrites filter signals as passive electrical cables (Rall 1959; Goldstein and Rall 1974), but were limited in their ability to apply directly to realistic morphologic data. Since then, applications of mathematical techniques (Fitzhugh 1961; Nagumo et al. 1962; Rinzel and Ermentrout 1989), advances in computational software (Bower and Beeman 1998; Carnevale and Hines 2006), model reduction (Clements and Redman 1989; Pinsky and Rinzel 1994), and computing power have resulted in models that have great potential for yielding insights into neuronal function. In particular, models have shown that morphology is a critical determinant of neuronal firing properties (Zador et al. 1995; Mainen and Sejnowski 1996; Vetter et al. 2001; Schaefer et al. 2003; Stiefel and Sejnowski 2007). The effects of morphology are further amplified by the actions of ion channels distributed throughout the dendrites (for review see Johnston and Narayanan 2008), both of which shape patterns of synaptic input. Our ability to understand neuronal function depends largely on analysis of the nonlinear interactions between morphology, electrical membrane properties, and synaptic input.

Electrotonic analysis—Electrotonic analysis (Rall 1969; Brown et al. 1992; Tsai et al. 1994; Carnevale et al. 1997) predicts how neuronal morphology interacts with passive membrane parameters (membrane capacitance C_m, specific membrane resistance R_m and axial resistivity R_a) to affect the propagation of electrical signals. For each point in the dendritic tree, the log attenuation L_{ij} is defined as the natural log of voltage attenuation from point i to point j. By computing L_{ij} everywhere throughout the dendrites, a neuron's anatomical structure can be transformed into an intuitive visual representation ("morphoelectrotonic transform"; Zador et al. 1995) of how that structure affects electrical signal transfer.

In a recent publication (Kabaso et al. 2009), we analyzed the electrotonic effects of age-related morphological changes in pyramidal neurons of the rhesus monkey PFC. Figure 6a shows the log attenuation of voltage flowing outward from the soma to the dendrites, for a layer 3 PFC pyramidal neuron from a young rhesus monkey (Kabaso et al. 2009). The log attenuation of voltage flowing inward from the dendrites toward the soma is defined similarly (Kabaso et al. 2009). Outward voltage attenuation in the apical dendrites was significantly reduced with age, both in "long" projection neurons from the superior temporal cortex to the PFC, and in "local" projection neurons within the PFC. In long projection neurons, inward voltage attenuation of apical dendrites was significantly reduced with age as well. Thus, if the age-related morphologic changes are not compensated by altered ion channel densities or kinetics, synaptic potentials would remain larger, and propagate more quickly, through the apical dendrites of old long projection neurons. Likewise, action potentials backpropagating through the apical dendrites of both long and local projection neurons would be larger and faster in old neurons. The reduction in spine densities with aging contributed strongly to our findings: voltage attenuation in the dendrites is not significantly different among the age groups when spine surface areas were not included (Kabaso et al. 2009).

Anomalous diffusion in dendrites and spines—At the fundamental microscopic level, cortical functioning is dependent on the diffusion of ions and other molecules that subserve electrical and chemical signaling in the brain. Important recent discoveries have revealed that the characteristics of this diffusion are altered by the morphology and

distribution of dendritic spines (Santamaria et al. 2006), and by the size and distribution of Aβ plaques (Mueggler et al. 2004; Banks and Fradin 2005). Both effects, trapping by dendritic spines and molecular crowding by amyloid plaques, result in anomalous subdiffusion in which the spatial variance grows as a sublinear power law in time (Metzler and Klafter 2000). In recent work, we introduced a new cable model for a cylindrical dendrite segment (Henry et al. 2008; Langlands et al. 2008, 2009) in which diffusion constants are replaced by timedependent operators with fractional-order exponents. We extended our derivation beyond the single dendrite level, demonstrating that anomalous subdiffusion of ions changes the electrotonic properties and firing rates of neurons (Langlands et al. 2009). Our studies are part of a larger effort to understand how spine morphologies and intracellular calcium dynamics affect signaling between dendrites and spines (Svoboda et al. 1996; Araya et al. 2006; Schmidt et al. 2007; Fedotov and Méndez 2008; Saftenku 2009; Schmidt and Eilers 2009). As reliable data on spine morphologies, intracellular calcium dynamics and ionic diffusion become increasingly available, equations describing anomalous subdiffusion will become more commonplace in computational modeling. These advances will lead to computational analyses of the effects of neurodegenerative changes to neurons on intracellular electrodiffusion.

Comparing active and morphological parameters—Computational studies often identify “active” parameters (those that control ionic membrane channels and intracellular calcium dynamics), which drive neuronal firing patterns, but discount the role of morphology (Goldman et al. 2001; Prinz et al. 2003, 2004; Olypher and Calabrese 2007; Taylor et al. 2009). We have used mathematical sensitivity analysis (Saltelli et al. 2000) to quantify how dendritic morphology affects neuronal firing patterns, and to compare these effects directly against those of active parameters (Weaver and Wearne 2008). Briefly, we perturb one parameter while keeping the rest constant, and define the sensitivity of an output to that parameter as the percentage change in output normalized by the percentage change in the parameter.

Figure 7a, b shows the sensitivity of spontaneous firing rate to parameter perturbations, for a model comprising a soma and unbranched cylindrical dendrite. For one combination of parameters called ‘Model 1’, the model fires action potentials spontaneously as shown by the solid black line of Fig. 7a. When the maximal conductance of the persistent sodium current $\bar{g}_{\mathrm{NaP}}$ was increased by 20% (Fig. 7a, thin red line), the firing rate increased by 50%; therefore the sensitivity of firing rate to $\bar{g}_{\mathrm{NaP}}$ was 50%/20% = +2.5. In contrast, reducing dendritic diameter by 20% increased firing rate by 67%, so that the sensitivity of firing rate to dendrite diameter was 67%/−20% = −3.35: a *larger* effect than that of $\bar{g}_{\mathrm{NaP}}$ which acts in the opposite direction. Importantly, these sensitivities depend greatly on the combination of active parameters used in the model, even among models with similar output (compare Fig. 7a, b). Both experimental (Chiba et al. 1992; Bucher et al. 2005; Swensen and Bean 2005; Schulz et al. 2006) and computational studies (Goldman et al. 2001; Prinz et al. 2003, 2004; Achard and De Schutter 2006; Weaver and Wearne 2008; Taylor et al. 2009) have shown that neurons can have similar outputs. Therefore, any sensitivity analysis must be carried out over a wide range of models consistent with experimental data. In doing this, we found some models for which dendrite diameter affected neuronal firing rate even more than the active parameters (Weaver and Wearne 2008). Extrapolating these results to the transgenic studies reviewed here suggests that the morphology of cortical neurons can contribute significantly to the observed physiology. It will be important to evaluate how the sensitivity of neuronal function to morphology and active parameters are affected by neurodegeneration. To do so, it is particularly important to have morphological and physiological data from the very same neurons. This work is ongoing within our research group (Yadav et al. 2008a, b, 2009). Application to the transgenic models described in this review will reveal more insight into the future.

Predicting compensations for morphological neurodegeneration—Perhaps, the most important application of sensitivity analysis to predict how parameters should compensate for one another to maintain a desired output (Olypher and Calabrese 2007; Weaver and Wearne 2008). Specifically, we have shown that perturbations of active parameters could counteract the effects of morphological changes (Weaver and Wearne 2008) like those that occur with neurodegeneration. As an example, Fig. 7c shows the effect of a 15% reduction in dendrite diameter on the firing rate of a morphologically faithful model of a precerebellar hindbrain neuron from goldfish (shown inset). Using the sensitivities of firing rate computed as described above, we predicted the precise perturbations needed of either $\bar{g}_{\mathrm{NaP}}$ (−11.3%) or of the A type potassium conductance $\bar{g}_{\mathrm{A}}$ (+25.4%) to compensate for the effect of the reduced diameter (Fig. 7d) (Weaver and Wearne 2008). We chose these parameters for compensations because neuronal firing rate was highly sensitive to them. Future compensatory predictions could be based on the experimental identification of active parameters that are most changed with neurodegeneration.

Application to transgenic mouse models—Our modeling results make several predictions that may apply to transgenic mouse models of neurodegeneration. First, changes in dendrite length, diameter, and spine densities/numbers in transgenic neurons compared to wildtype neurons may significantly impact the attenuation of signals to and from the soma. This may happen over an entire neuron, or in limited regions, such as dendrites passing through or near fibrillar amyloid deposits, or in apical tufts that undergo atrophy. Long projection neurons are particularly vulnerable in AD (Hof et al. 1990; Bussiére et al. 2003; Hof and Morrison 2004), giving greater weight to the significant differences in voltage attenuation observed in long projection neurons (Kabaso et al. 2009). Second, changes in spine density may affect the diffusion rate of intracellular messengers and ions. Elongated dendrites may result in less trapping of electrical and chemical signals within spines; this phenomenon may be functionally significant. We must also consider how spine loss might impact the amount of excitatory input that a neuron receives. Finally, it is likely that interactions between morphology and active parameters vary between wild-type and transgenic neurons. To study this more fully we must measure both detailed morphological properties and ionic currents in wild-type and transgenic neurons. To evaluate the degree to which these predictions truly apply to the transgenic mouse models, we will apply the mathematical methods described here directly to the transgenic data that we have collected. These computational studies will likely lead to explicit predictions of which parameters to change, and by how much, to counteract morphological changes that affect physiological function in neurodegenerative disease.

Acknowledgments

We thank Dr B.I. Henry and all the members of the Wearne, Luebke, and Hof laboratories for their participation in these studies. This work was supported by NIH Grants AG00001, AG02219, AG05138, AG025062, MH58911, MH071818, DC05669, and Australian Research Council Discovery Grant DP0665482.

References

Achard P, De Schutter E. Complex parameter landscape for a complex neuron model. PLoS Comput Biol 2006;2(7):e94. [PubMed: 16848639]

Al-Kofahi KA, Lasek S, Szarowski DH, Pace CJ, Nagy G, Turner JN, Roysam B. Rapid automated three-dimensional tracing of neurons from confocal image stacks. IEEE Trans Inf Technol Biomed 2002;6(2):171–187. [PubMed: 12075671]

Alvarez VA, Sabatini BL. Anatomical and physiological plasticity of dendritic spines. Annu Rev Neurosci 2007;30:79–97. [PubMed: 17280523]

Anderton BH, Callahan L, Coleman P, Davies P, Flood D, Jicha GA, Ohm T, Weaver C. Dendritic changes in Alzheimer's disease and factors that may underlie these changes. Prog Neurobiol 1998;55(6):595–609. [PubMed: 9670220]

Andorfer C, Acker CM, Kress Y, Hof PR, Duff K, Davies P. Cell-cycle reentry and cell death in transgenic mice expressing nonmutant human tau isoforms. J Neurosci 2005;25(22):5446–5454. [PubMed: 15930395]

Araya R, Jiang J, Eisenthal KB, Yuste R. The spine neck filters membrane potentials. Proc Natl Acad Sci USA 2006;103(47):17961–17966. [PubMed: 17093040]

Ascoli GA. Passive dendritic integration heavily affects spiking dynamics of recurrent networks. Neural Netw 2003;16(5–6):657–663. [PubMed: 12850020]

Baer SM, Rinzel J. Propagation of dendritic spikes mediated by excitable spines: a continuum theory. J Neurophysiol 1991;65(4):874– 890. [PubMed: 2051208]

Banks DS, Fradin C. Anomalous diffusion of proteins due to molecular crowding. Biophys J 2005;89(5):2960–2971. [PubMed: 16113107]

Bekkers JM, Hausser M. Targeted dendrotomy reveals active and passive contributions of the dendritic tree to synaptic integration and neuronal output. Proc Natl Acad Sci USA 2007;104(27):11447–11452. [PubMed: 17592119]

Berger T, Larkum ME, Luscher HR. High I(h) channel density in the distal apical dendrite of layer V pyramidal cells increases bidirectional attenuation of EPSPs. J Neurophysiol 2001;85(2):855–868. [PubMed: 11160518]

Bernander O, Douglas RJ, Martin KA, Koch C. Synaptic background activity influences spatiotemporal integration in single pyramidal cells. Proc Natl Acad Sci USA 1991;88(24):11569–11573. [PubMed: 1763072]

Bhatt DH, Zhang S, Gan WB. Dendritic spine dynamics. Annu Rev Physiol 2009;71:261–282. [PubMed: 19575680]

Biscaro B, Lindvall O, Hock C, Ekdahl CT, Nitsch RM. Abeta immunotherapy protects morphology and survival of adult-born neurons in doubly transgenic APP/PS1 mice. J Neurosci 2009;29(45):14108–14119. [PubMed: 19906959]

Bloodgood BL, Sabatini BL. Neuronal activity regulates diffusion across the neck of dendritic spines. Science 2005;310(5749):866–869. [PubMed: 16272125]

Bloodgood BL, Sabatini BL. Ca^{2+} signaling in dendritic spines. Curr Opin Neurobiol 2007;17(3):345–351. [PubMed: 17451936]

Bourne J, Harris KM. Do thin spines learn to be mushroom spines that remember? Curr Opin Neurobiol 2007;17(3):381–386. [PubMed: 17498943]

Bower, JM.; Beeman, D. The book of genesis: exploring realistic neural models with the general neural simulation system. Springer; New York: 1998.

Brown, TH.; Zador, A.; Mainen, ZF.; Claiborne, BJ. Hebbian computations in hippocampal dendrites and spines. In: McKenna, T.; Davis, J.; Zornetzer, SF., editors. Single neuron computation. Academic Press; San Diego: 1992. p. 81-116.

Brown JT, Richardson JC, Collingridge GL, Randall AD, Davies CH. Synaptic transmission and synchronous activity is disrupted in hippocampal slices taken from aged TAS10 mice. Hippocampus 2005;15(1):110–117. [PubMed: 15390159]

Bucher D, Prinz AA, Marder E. Animal-to-animal variability in motor pattern prediction in adults and during growth. J Neurosci 2005;25:1611–1619. [PubMed: 15716396]

Buhl EH, Lübke J. Intracellular lucifer yellow injection in fixed brain slices combined with retrograde tracing, light and electron microscopy. Neuroscience 1989;28(1):3–16. [PubMed: 2668782]

Bussiére T, Giannakopoulos P, Bouras C, Perl DP, Morrison JH, Hof PR. Progressive degeneration of nonphosphorylated neurofilament protein-enriched pyramidal neurons predicts cognitive impairment in Alzheimer's disease: stereologic analysis of prefrontal cortex area 9. J Comp Neurol 2003;463(3):281–302. [PubMed: 12820162]

Capowski, JJ. The microcomputer in cell and neurobiology research. Elsevier; Amsterdam: 1985.

Carnevale, NT.; Hines, ML. The neuron book. Cambridge University Press; Cambridge: 2006.

Carnevale NT, Tsai KY, Claiborne BJ, Brown TH. Comparative electrotonic analysis of three classes of rat hippocampal neurons. J Neurophysiol 1997;78:703–720. [PubMed: 9307106]

Caserta F, Eldred WD, Fernandez E, Hausman RE, Stanford LR, Bulderev SV, Schwarzer S, Stanley HE. Determination of fractal dimension of physiologically characterized neurons in two and three dimensions. J Neurosci Methods 1995;56:133– 144. [PubMed: 7752679]

Chapman PF, White GL, Jones MW, Cooper-Blacketer D, Marshall VJ, Irizarry M, Younkin L, Good MA, Bliss TV, Hyman BT, Younkin SG, Hsiao KK. Impaired synaptic plasticity and learning in aged amyloid precursor protein transgenic mice. Nat Neurosci 1999;2(3):271–276. [PubMed: 10195221]

Cheng J, Zhou X, Miller E, Witt RM, Zhu J, Sabatini BL, Wong ST. A novel computational approach for automatic dendrite spines detection in two-photon laser scan microscopy. J Neurosci Methods 2007;165(1):122–134. [PubMed: 17629570]

Chiba A, Kamper G, Murphey RK. Response properties of interneurons of the cricket cercal sensory system are conserved in spite of changes in peripheral receptors during maturation. J Exp Biol 1992;164:205–226.

Clements JD, Redman SJ. Cable properties of cat spinal motoneurones measured by combining voltage clamp, current clamp and intracellular staining. J Physiol 1989;409:63–87. [PubMed: 2585300]

Conde C, Caceres A. Microtubule assembly, organization and dynamics in axons and dendrites. Nat Rev Neurosci 2009;10(5):319–332. [PubMed: 19377501]

Duan H, Wearne SL, Rocher AB, Macedo A, Morrison JH, Hof PR. Age-related dendritic and spine changes in corticocortically projecting neurons in macaque monkeys. Cereb Cortex 2003;13(9): 950–961. [PubMed: 12902394]

Duff K, Suleman F. Transgenic mouse models of Alzheimer's disease: how useful have they been for therapeutic development? Brief Funct Genomic Proteomic 2004;3(1):47–59. [PubMed: 15163359]

Duyckaerts C, Potier MC, Delatour B. Alzheimer disease models and human neuropathology: similarities and differences. Acta Neuropathol 2008;115(1):5–38. [PubMed: 18038275]

Euler T, Denk W. Dendritic processing. Curr Opin Neurobiol 2001;11(4):415–422. [PubMed: 11502386]

Falke E, Nissanov J, Mitchell TW, Bennett DA, Trojanowski JQ, Arnold SE. Subicular dendritic arborization in Alzheimer's disease correlates with neurofibrillary tangle density. Am J Pathol 2003;163(4):1615–1621. [PubMed: 14507668]

Fedotov S, Méndez V. Non-Markovian model for transport and reactions of particles in spiny dendrites. Phys Rev Lett 2008;101(21):218102. [PubMed: 19113454]

Feldmeyer D, Lubke J, Silver RA, Sakmann B. Synaptic connections between layer 4 spiny neurone-layer 2/3 pyramidal cell pairs in juvenile rat barrel cortex: physiology and anatomy of interlaminar signalling within a cortical column. J Physiol 2002;538(Pt 3):803–822. [PubMed: 11826166]

Ferrer I, Guionnet N, Cruz-Sanchez F, Tunon T. Neuronal alterations in patients with dementia: a Golgi study on biopsy samples. Neurosci Lett 1990;114(1):11–16. [PubMed: 2199862]

Fitzhugh R. Impulses and physiological states in theoretical models of nerve membrane. Biophys J 1961;1:445–466. [PubMed: 19431309]

Fitzjohn SM, Morton RA, Kuenzi F, Rosahl TW, Shearman M, Lewis H, Smith D, Reynolds DS, Davies CH, Collingridge GL, Seabrook GR. Age-related impairment of synaptic transmission but normal long-term potentiation in transgenic mice that overexpress the human APP695SWE mutant form of amyloid precursor protein. J Neurosci 2001;21(13):4691–4698. [PubMed: 11425896]

Flood DG. Region-specific stability of dendritic extent in normal human aging and regression in Alzheimer's disease. II. Subiculum. Brain Res 1991;540(1–2):83–95. [PubMed: 2054635]

Garcia-Lopez P, Garcia-Marin V, Freire M. The discovery of dendritic spines by Cajal in 1888 and its relevance in the present neuroscience. Prog Neurobiol 2007;83(2):110–130. [PubMed: 17681416]

Garcia-Marin V, Garcia-Lopez P, Freire M. Cajal's contributions to the study of Alzheimer's disease. J Alzheimers Dis 2007;12(2):161–174. [PubMed: 17917161]

Gertz HJ, Kruger H, Patt S, Cervos-Navarro J. Tangle-bearing neurons show more extensive dendritic trees than tangle-free neurons in area CA1 of the hippocampus in Alzheimer's disease. Brain Res 1991;548(1–2):260–266. [PubMed: 1714332]

Giacchino J, Criado JR, Games D, Henriksen S. In vivo synaptic transmission in young and aged amyloid precursor protein transgenic mice. Brain Res 2000;876(1–2):185–190. [PubMed: 10973607]

Giannakopoulos P, Kövari E, Gold G, von Gunten A, Hof PR, Bouras C. Pathological substrates of cognitive decline in Alzheimer's disease. Front Neurol Neurosci 2009;24:20–29. [PubMed: 19182459]

Goldman MS, Golowasch J, Marder E, Abbott LF. Global structure, robustness, and modulation of neuronal models. J Neurosci 2001;21(14):5229–5238. [PubMed: 11438598]

Goldstein SS, Rall W. Changes of action potential shape and velocity for changing core conductor geometry. Biophys J 1974;14(10):731–757. [PubMed: 4420585]

Grutzendler J, Kasthuri N, Gan WB. Long-term dendritic spine stability in the adult cortex. Nature 2002;420(6917):812–816. [PubMed: 12490949]

Hall GF, Chu B, Lee G, Yao J. Human tau filaments induce microtubule and synapse loss in an in vivo model of neurofibrillary degenerative disease. J Cell Sci 2000;113(Pt 8):1373–1387. [PubMed: 10725221]

Hall GF, Lee VM, Lee G, Yao J. Staging of neurofibrillary degeneration caused by human tau overexpression in a unique cellular model of human tauopathy. Am J Pathol 2001;158(1):235–246. [PubMed: 11141497]

Halpain S, Spencer K, Graber S. Dynamics and pathology of dendritic spines. Prog Brain Res 2005;147:29–37. [PubMed: 15581695]

Hartley DM, Walsh DM, Ye CP, Diehl T, Vasquez S, Vassilev PM, Teplow DB, Selkoe DJ. Protofibrillar intermediates of amyloid beta-protein induce acute electrophysiological changes and progressive neurotoxicity in cortical neurons. J Neurosci 1999;19(20):8876–8884. [PubMed: 10516307]

Hausser M, Spruston N, Stuart GJ. Diversity and dynamics of dendritic signaling. Science 2000;290(5492):739–744. [PubMed: 11052929]

He W, Hamilton TA, Cohen AR, Holmes TJ, Pace C, Szarowski DH, Turner JN, Roysam B. Automated three-dimensional tracing of neurons in confocal and bright field images. Microsc Microanal 2003;9(4):296–310. [PubMed: 12901764]

Henry, BI.; Hof, PR.; Rothnie, P.; Wearne, SL. Fractal analysis of aggregates of non-uniformly sized particles: an application to macaque monkey cortical pyramidal neurons. In: Novak, MM., editor. Emergent nature: patterns, growth and scaling in the sciences. World Scientific Publishing; Singapore: 2002. p. 65-75.

Henry BI, Langlands TA, Wearne SL. Fractional cable models for spiny neuronal dendrites. Phys Rev Lett 2008;100(12):128103. [PubMed: 18517914]

Hering H, Sheng M. Dendritic spines: structure, dynamics and regulation. Nat Rev Neurosci 2001;2(12):880–888. [PubMed: 11733795]

Hodgkin AL, Huxley AF. A quantitative description of membrane current and its application to conduction and excitation in nerve. J Physiol 1952;117:500–544. [PubMed: 12991237]

Hof PR, Morrison JH. The aging brain: morphomolecular senescence of cortical circuits. Trends Neurosci 2004;27:607–613. [PubMed: 15374672]

Hof PR, Cox K, Morrison JH. Quantitative analysis of a vulnerable subset of pyramidal neurons in Alzheimer's disease. I. Superior frontal and inferior temporal cortex. J Comp Neurol 1990;301:44–54. [PubMed: 2127598]

Holthoff K, Tsay D, Yuste R. Calcium dynamics of spines depend on their dendritic location. Neuron 2002;33(3):425–437. [PubMed: 11832229]

Holtmaat A, Svoboda K. Experience-dependent structural synaptic plasticity in the mammalian brain. Nat Rev Neurosci 2009;10(9):647–658. [PubMed: 19693029]

Holtmaat AJ, Trachtenberg JT, Wilbrecht L, Shepherd GM, Zhang X, Knott GW, Svoboda K. Transient and persistent dendritic spines in the neocortex in vivo. Neuron 2005;45(2):279–291. [PubMed: 15664179]

Hsia AY, Masliah E, McConlogue L, Yu GQ, Tatsuno G, Hu K, Kholodenko D, Malenka RC, Nicoll RA, Mucke L. Plaque-independent disruption of neural circuits in Alzheimer's disease mouse models. Proc Natl Acad Sci USA 1999;96(6):3228–3233. [PubMed: 10077666]

Hsiao K, Chapman P, Nilsen S, Eckman C, Harigaya Y, Younkin S, Yang F, Cole G. Correlative memory deficits, Aβelevation, and amyloid plaques in transgenic mice. Science 1996;274(5284): 99–102. [PubMed: 8810256]

Jaslove SW. The integrative properties of spiny distal dendrites. Neuroscience 1992;47(3):495–519. [PubMed: 1584406]

Jelinek HF, Elston GN. Pyramidal neurones in macaque visual cortex: interareal phenotypic variation of dendritic branching patterns. Fractals 2001;9:297–303.

Johnston D, Narayanan R. Active dendrites: colorful wings of the mysterious butterflies. Trends Neurosci 2008;31(6):309–316. [PubMed: 18471907]

Johnston D, Magee JC, Colbert CM, Cristie BR. Active properties of neuronal dendrites. Annu Rev Neurosci 1996;19:165–186. [PubMed: 8833440]

Kabaso D, Coskren PJ, Henry BI, Hof PR, Wearne SL. The electrotonic structure of pyramidal neurons contributing to prefrontal cortical circuits in macaque monkeys is significantly altered in aging. Cereb Cortex 2009;19(10):2248–2268. [PubMed: 19150923]

Kamenetz F, Tomita T, Hsieh H, Seabrook G, Borchelt D, Iwatsubo T, Sisodia S, Malinow R. APP processing and synaptic function. Neuron 2003;37(6):925–937. [PubMed: 12670422]

Kampa BM, Letzkus JJ, Stuart GJ. Dendritic mechanisms controlling spike-timing-dependent synaptic plasticity. Trends Neurosci 2007;30(9):456–463. [PubMed: 17765330]

Kasai H, Matsuzaki M, Noguchi J, Yasumatsu N, Nakahara H. Structure–stability–function relationships of dendritic spines. Trends Neurosci 2003;26(7):360–368. [PubMed: 12850432]

Klyubin I, Walsh DM, Cullen WK, Fadeeva JV, Anwyl R, Selkoe DJ, Rowan MJ. Soluble Arctic amyloid beta protein inhibits hippocampal long-term potentiation in vivo. Eur J Neurosci 2004;19(10):2839–2846. [PubMed: 15147317]

Knobloch M, Mansuy IM. Dendritic spine loss and synaptic alterations in Alzheimer's disease. Mol Neurobiol 2008;37(1):73–82. [PubMed: 18438727]

Knowles RB, Wyart C, Buldyrev SV, Cruz L, Urbanc B, Hasselmo ME, Stanley HE, Hyman BT. Plaque-induced neurite abnormalities: implications for disruption of neural networks in Alzheimer's disease. Proc Natl Acad Sci USA 1999;96(9):5274–5279. [PubMed: 10220456]

Koch C, Segev I. The role of single neurons in information processing. Nat Neurosci 2000;3(Suppl): 1171–1177. [PubMed: 11127834]

Koh IY, Lindquist WB, Zito K, Nimchinsky EA, Svoboda K. An image analysis algorithm for dendritic spines. Neural Comput 2002;14(6):1283–1310. [PubMed: 12020447]

Krichmar JL, Nasuto SJ, Scorcioni R, Washington SD, Ascoli GA. Effects of dendritic morphology on CA3 pyramidal cell electrophysiology: a simulation study. Brain Res 2002;941(1–2):11–28. [PubMed: 12031543]

Kuchibhotla KV, Goldman ST, Lattarulo CR, Wu HY, Hyman BT, Bacskai BJ. Abeta plaques lead to aberrant regulation of calcium homeostasis in vivo resulting in structural and functional disruption of neuronal networks. Neuron 2008;59(2):214–225. [PubMed: 18667150]

Langlands TA, Henry BI, Wearne SL. Anomalous subdiffusion with multispecies linear reaction dynamics. Phys Rev E Stat Nonlin Soft Matter Phys 2008;77(2 Pt 1):021111. [PubMed: 18351991]

Langlands TA, Henry BI, Wearne SL. Fractional cable equation models for anomalous electrodiffusion in nerve cells: infinite domain solutions. J Math Biol 2009;59(6):761–808. [PubMed: 19221755]

Larson J, Lynch G, Games D, Seubert P. Alterations in synaptic transmission and long-term potentiation in hippocampal slices from young and aged PDAPP mice. Brain Res 1999;840(1– 2): 23–35. [PubMed: 10517949]

Le R, Cruz L, Urbanc B, Knowles RB, Hsiao-Ashe K, Duff K, Irizarry MC, Stanley HE, Hyman BT. Plaque-induced abnormalities in neurite geometry in transgenic models of Alzheimer disease: implications for neural system disruption. J Neuropathol Exp Neurol 2001;60(8):753–758. [PubMed: 11487049]

Lendvai B, Stern EA, Chen B, Svoboda K. Experiencedependent plasticity of dendritic spines in the developing rat barrel cortex in vivo. Nature 2000;404(6780):876–881. [PubMed: 10786794]

Lewis, J.; Hutton, M. Animal models of tauopathies atypical parkinsonian disorders. Litvan, I., editor. Humana Press; Totowa: 2005. p. 65-76.

Liu X, Erikson C, Brun A. Cortical synaptic changes and gliosis in normal aging, Alzheimer's disease and frontal lobe degeneration. Dementia 1996;7(3):128–134. [PubMed: 8740626]

Lombardo JA, Stern EA, McLellan ME, Kajdasz ST, Hickey GA, Bacskai BJ, Hyman BT. Amyloid-beta antibody treatment leads to rapid normalization of plaque-induced neuritic alterations. J Neurosci 2003;23:10879–10883. [PubMed: 14645482]

Lorincz A, Notomi T, Tamas G, Shigemoto R, Nusser Z. Polarized and compartment-dependent distribution of HCN1 in pyramidal cell dendrites. Nat Neurosci 2002;5(11):1185–1193. [PubMed: 12389030]

Lubke J, Egger V, Sakmann B, Feldmeyer D. Columnar organization of dendrites and axons of single and synaptically coupled excitatory spiny neurons in layer 4 of the rat barrel cortex. J Neurosci 2000;20(14):5300–5311. [PubMed: 10884314]

Magee JC, Johnston D. Plasticity of dendritic function. Curr Opin Neurobiol 2005;15(3):334–342. [PubMed: 15922583]

Mainen ZF, Sejnowski TJ. Influence of dendritic structure on firing pattern in model neocortical neurons. Nature 1996;382(6589):363–366. [PubMed: 8684467]

Matus A. Growth of dendritic spines: a continuing story. Curr Opin Neurobiol 2005;15(1):67–72. [PubMed: 15721746]

Matus A, Shepherd GM. The millennium of the dendrite? Neuron 2000;27(3):431–434. [PubMed: 11055426]

Metzler R, Klafter J. Subdiffusive transport close to thermal equilibrium: from the Langevin equation to fractional diffusion. Phys Rev E Stat Phys Plasmas Fluids Relat Interdiscip Topics 2000;61(6 Pt A):6308–6311. [PubMed: 11088305]

Migliore M, Shepherd GM. Emerging rules for the distributions of active dendritic conductances. Nat Rev Neurosci 2002;3(5):362–370. [PubMed: 11988775]

Mocanu MM, Nissen A, Eckermann K, Khlistunova I, Biernat J, Drexler D, Petrova O, Schonig K, Bujard H, Mandelkow E, Zhou L, Rune G, Mandelkow EM. The potential for betastructure in the repeat domain of tau protein determines aggregation, synaptic decay, neuronal loss, and coassembly with endogenous Tau in inducible mouse models of tauopathy. J Neurosci 2008;28(3):737–748. [PubMed: 18199773]

Moolman DL, Vitolo OV, Vonsattel JP, Shelanski ML. Dendrite and dendritic spine alterations in Alzheimer models. J Neurocytol 2004;33(3):377–387. [PubMed: 15475691]

Morrison JH, Hof PR. Life and death of neurons in the aging brain. Science 1997;278(5337):412–419. [PubMed: 9334292]

Morrison JH, Hof PR. Selective vulnerability of corticocortical and hippocampal circuits in aging and Alzheimer's disease. Prog Brain Res 2002;136:467–486. [PubMed: 12143403]

Mueggler T, Meyer-Luehmann M, Rausch M, Staufenbiel M, Jucker M, Rudin M. Restricted diffusion in the brain of transgenic mice with cerebral amyloidosis. Eur J Neurosci 2004;20(3):811–817. [PubMed: 15255991]

Myatt, DR.; Nasuto, SJ.; Maybank, SJ. Towards the automatic reconstruction of dendritic trees using particle filters. Nonlinear Statistical Signal Processing Workshop, IEEE; 13– 15 Sept 2006; 2006. p. 193-196.

Nagumo JS, Arimato S, Yoshizawa S. An active pulse transmission line simulating a nerve axon. Proc IRE 1962;50:2061–2070.

Neher E, Sakmann B. Single-channel currents recorded from membrane of denervated frog muscle fibres. Nature 1976;260(5554):799–802. [PubMed: 1083489]

Nimchinsky EA, Sabatini BL, Svoboda K. Structure and function of dendritic spines. Annu Rev Physiol 2002;64:313–353. [PubMed: 11826272]

Nusser Z. Variability in the subcellular distribution of ion channels increases neuronal diversity. Trends Neurosci 2009;32(5):267–274. [PubMed: 19299025]

Nusser Z, Lujan R, Laube G, Roberts JD, Molnar E, Somogyi P. Cell type and pathway dependence of synaptic AMPA receptor number and variability in the hippocampus. Neuron 1998;21(3):545–559. [PubMed: 9768841]

Olypher AV, Calabrese RL. Using constraints on neuronal activity to reveal compensatory changes in neuronal parameters. J Neurophysiol 2007;98(6):3749–3758. [PubMed: 17855581]

Paula-Barbosa MM, Cardoso RM, Guimaraes ML, Cruz C. Dendritic degeneration and regrowth in the cerebral cortex of patients with Alzheimer's disease. J Neurol Sci 1980;45(1):129–134. [PubMed: 7359162]

Pinsky PF, Rinzel J. Intrinsic and network rhythmogenesis in a reduced Traub model for CA3 neurons. J Comp Neurosci 1994;1:39–60.

Prinz AA, Billimoria CP, Marder E. Alternative to hand-tuning conductance-based models: construction and analysis of databases of model neurons. J Neurophysiol 2003;90(6):3998–4015. [PubMed: 12944532]

Prinz AA, Bucher D, Marder E. Similar network activity from disparate circuit parameters. Nat Neurosci 2004;7(12):1345–1352. [PubMed: 15558066]

Probst A, Basler V, Bron B, Ulrich J. Neuritic plaques in senile dementia of Alzheimer type: a Golgi analysis in the hippocampal region. Brain Res 1983;268(2):249–254. [PubMed: 6191831]

Rall W. Branching dendritic trees and motoneuron membrane resistivity. Exp Neurol 1959;1:491–527. [PubMed: 14435979]

Rall W. Time constants and electrotonic length of membrane cylinders and neurons. Biophys J 1969;9:1483–1508. [PubMed: 5352228]

Ramón, y; Cajal, S. Histologie du systeme nerveux de l'homme et des vertébrés. Masson; Paris: 1911.

Rho JH, Sidman RL. Intracellular injection of lucifer yellow into lightly fixed cerebellar neurons. Neurosci Lett 1986;72(1):21–24. [PubMed: 2433645]

Ridler TW, Calvard S. Picture thresholding using an iterative selection method. IEEE Trans Syst Man Cybern SMC 1978;8:630–632.

Rinzel, J.; Ermentrout, GB. Analysis of neuronal excitability and oscillations. In: Koch, C.; Segev, I., editors. Methods in neuronal modeling: from ions to networks. The MIT Press; Cambridge: 1989. p. 251-291.

Rocher AB, Kinson MS, Luebke JI. Significant structural but not physiological changes in cortical neurons of 12-month-old Tg2576 mice. Neurobiol Dis 2008;32(2):309–318. [PubMed: 18721884]

Rocher AB, Crimins JL, Amatrudo JM, Kinson MS, Todd-Brown MA, Lewis J, Luebke JI. Structural and functional changes in tau mutant mice neurons are not linked to the presence of NFTs. Exp Neurol. 2009 [Epub ahead of print].

Rockland KS, Pandya DN. Laminar origins and terminations of cortical connections of the occipital lobe in the rhesus monkey. Brain Res 1979;179(1):3–20. [PubMed: 116716]

Roder S, Danober L, Pozza MF, Lingenhoehl K, Wiederhold KH, Olpe HR. Electrophysiological studies on the hippocampus and prefrontal cortex assessing the effects of amyloidosis in amyloid precursor protein 23 transgenic mice. Neuroscience 2003;120(3):705–720. [PubMed: 12895511]

Rodriguez A, Ehlenberger D, Kelliher K, Einstein M, Henderson SC, Morrison JH, Hof PR, Wearne SL. Automated reconstruction of three-dimensional neuronal morphology from laser scanning microscopy images. Methods 2003;30(1):94–105. [PubMed: 12695107]

Rodriguez A, Ehlenberger DB, Hof PR, Wearne SL. Rayburst sampling, an algorithm for automated three-dimensional shape analysis from laser scanning microscopy images. Nat Protoc 2006;1(4): 2152–2161. [PubMed: 17487207]

Rodriguez A, Ehlenberger DB, Dickstein DL, Hof PR, Wearne SL. Automated three-dimensional detection and shape classification of dendritic spines from fluorescence microscopy images. PLoS One 2008;3(4):e1997. [PubMed: 18431482]

Rodriguez A, Ehlenberger DB, Hof PR, Wearne SL. Threedimensional neuron tracing by voxel scooping. J Neurosci Methods 2009;184(1):169–175. [PubMed: 19632273]

Rothnie P, Kabaso D, Hof PR, Henry BI, Wearne SL. Functionally relevant measures of spatial complexity in neuronal dendritic arbors. J Theor Biol 2006;238(3):505–526. [PubMed: 16083911]

Rozkalne A, Spires-Jones TL, Stern EA, Hyman BT. A single dose of passive immunotherapy has extended benefits on synapses, neuritis in an Alzheimer's disease mouse model. Brain Res 2009;1280:178–185. [PubMed: 19465012]

Saftenku EE. Computational study of non-homogeneous distribution of Ca^{2+} handling systems in cerebellar granule cells. J Theor Biol 2009;257(2):228–244. [PubMed: 19121636]

Saltelli, A.; Chan, K.; Scott, EM., editors. Sensitivity analysis. Wiley; New York: 2000.

Samsonovich AV, Ascoli GA. Morphological homeostasis in cortical dendrites. Proc Natl Acad Sci USA 2006;103(5):1569–1574. [PubMed: 16418293]

Santacruz K, Lewis J, Spires T, Paulson J, Kotilinek L, Ingelsson M, Guimaraes A, DeTure M, Ramsden M, McGowan E, Forster C, Yue M, Orne J, Janus C, Mariash A, Kuskowski M, Hyman B, Hutton M, Ashe KH. Tau suppression in a neurodegenerative mouse model improves memory function. Science 2005;309(5733):476–481. [PubMed: 16020737]

Santamaria F, Wils S, De Schutter E, Augustine GJ. Anomalous diffusion in Purkinje cell dendrites caused by spines. Neuron 2006;52(4):635–648. [PubMed: 17114048]

Santamaria-Pang A, Colbert CM, Saggau P, Kakadiaris IA. Automatic centerline extraction of irregular tubular structures using probability volumes from multiphoton imaging. Int Conf Med Image Comput Comput Assist Interv 2007;10(Pt 2):486–494.

Schaefer AT, Larkum ME, Sakmann B, Roth A. Coincidence detection in pyramidal neurons is tuned by their dendritic branching pattern. J Neurophysiol 2003;89(6):3143–3154. [PubMed: 12612010]

Schikorski T, Stevens CF. Quantitative fine-structural analysis of olfactory cortical synapses. Proc Natl Acad Sci USA 1999;96(7):4107–4112. [PubMed: 10097171]

Schindowski K, Bretteville A, Leroy K, Begard S, Brion JP, Hamdane M, Buee L. Alzheimer's disease-like tau neuropathology leads to memory deficits and loss of functional synapses in a novel mutated tau transgenic mouse without any motor deficits. Am J Pathol 2006;169(2):599–616. [PubMed: 16877359]

Schmidt H, Eilers J. Spine neck geometry determines spinodendritic cross-talk in the presence of mobile endogenous calcium binding proteins. J Comput Neurosci 2009;27(2):229–243. [PubMed: 19229604]

Schmidt H, Kunerth S, Wilms C, Strotmann R, Eilers J. Spinodendritic cross-talk in rodent Purkinje neurons mediated by endogenous Ca^{2+}-binding proteins. J Physiol 2007;581(Pt 2):619–629. [PubMed: 17347272]

Schmitt S, Evers JF, Duch C, Scholz M, Obermayer K. New methods for the computer-assisted 3-D reconstruction of neurons from confocal image stacks. Neuroimage 2004;23(4):1283–1298. [PubMed: 15589093]

Schulz DJ, Goaillard JM, Marder E. Variable channel expression in identified single and electrically coupled neurons in different animals. Nat Neurosci 2006;9:356–362. [PubMed: 16444270]

Scorcioni, R.; Ascoli, GA. Algorithmic extraction of morphological statistics from electronic archives of neuroanatomy. In: Mira, J.; Prieto, A., editors. Lecture notes in computer science. Springer; Berlin: 2001. p. 30-37.

Scott SA. Dendritic atrophy and remodeling of amygdaloid neurons in Alzheimer's disease. Dementia 1993;4(5):264–272. [PubMed: 7505158]

Segev I, London M. Untangling dendrites with quantitative models. Science 2000;290(5492):744–750. [PubMed: 11052930]

Sholl DA. Dendritic organization in the neurons of the visual and motor cortices of the cat. J Anat 1953;87:387–406. [PubMed: 13117757]

Smith TG, Marks WB, Lange GD, Sheriff JWH, Neale EA. A fractal analysis of cell images. J Neurosci Methods 1989;27:173–180. [PubMed: 2709885]

Smith DL, Pozueta J, Gong B, Arancio O, Shelanski M. Reversal of long-term dendritic spine alterations in Alzheimer disease models. Proc Natl Acad Sci USA 2009;106(39):16877–16882. [PubMed: 19805389]

Spires TL, Hyman BT. Neuronal structure is altered by amyloid plaques. Rev Neurosci 2004;15(4):267–278. [PubMed: 15526551]

Spires TL, Meyer-Luehmann M, Stern EA, McLean PJ, Skoch J, Nguyen PT, Bacskai BJ, Hyman BT. Dendritic spine abnormalities in amyloid precursor protein transgenic mice demonstrated by gene transfer and intravital multiphoton microscopy. J Neurosci 2005;25(31):7278–7287. [PubMed: 16079410]

Spires-Jones TL, Stoothoff WH, de Calignon A, Jones PB, Hyman BT. Tau pathophysiology in neurodegeneration: a tangled issue. Trends Neurosci 2009;32(3):150–159. [PubMed: 19162340]

Spruston N. Pyramidal neurons: dendritic structure and synaptic integration. Nat Rev Neurosci 2008;9(3):206–221. [PubMed: 18270515]

Stern EA, Bacskai BJ, Hickey GA, Attenello FJ, Lombardo JA, Hyman BT. Cortical synaptic integration in vivo is disrupted by amyloid-beta plaques. J Neurosci 2004;24(19):4535–4540. [PubMed: 15140924]

Stiefel KM, Sejnowski TJ. Mapping function onto neuronal morphology. J Neurophysiol 2007;98(1): 513–526. [PubMed: 17428904]

Stratford, K.; Mason, A.; Larkman, AU.; Major, G.; Jack, JJB. The modelling of pyramidal neurones in the visual cortex. In: Durbin, R.; Miall, C.; Mitchison, G., editors. The computing neuron. Addison- Wesley; Wokingham: 1989. p. 296-321.

Streekstra GJ, van Pelt J. Analysis of tubular structures in three-dimensional confocal images. Network 2002;13(3):381–395. [PubMed: 12222820]

Stuart, G.; Spruston, N. Dendrites. Oxford University Press; Oxford: 2007.

Stuart G, Spruston N, Sakmann B, Hausser M. Action potential initiation and backpropagation in neurons of the mammalian CNS. Trends Neurosci 1997;20(3):125–131. [PubMed: 9061867]

Surkis A, Peskin CS, Tranchina D, Leonard CS. Recovery of cable properties through active and passive modeling of subthreshold membrane responses from laterodorsal tegmental neurons. J Neurophysiol 1998;80(5):2593–2607. [PubMed: 9819266]

Svoboda K, Tank DW, Denk W. Direct measurement of coupling between dendritic spines and shafts. Science 1996;272(5262):716–719. [PubMed: 8614831]

Swensen AM, Bean BP. Robustness of burst firing in dissociated purkinje neurons with acute or long-term reductions in sodium conductance. J Neurosci 2005;25(14):3509–3520. [PubMed: 15814781]

Tackenberg C, Ghori A, Brandt R. Thin, stubby or mushroom: spine pathology in Alzheimer's disease. Curr Alzheimer Res 2009;6(3):261–268. [PubMed: 19519307]

Taylor AL, Goaillard JM, Marder E. How multiple conductances determine electrophysiological properties in a multicompartment model. J Neurosci 2009;29(17):5573–5586. [PubMed: 19403824]

Thierry AM, Godbout R, Mantz J, Glowinski J. Influence of the ascending monoaminergic systems on the activity of the rat prefrontal cortex. Prog Brain Res 1990;85:357–364. discussion 364–365. [PubMed: 2094905]

Trachtenberg JT, Chen BE, Knott GW, Feng G, Sanes JR, Welker E, Svoboda K. Long-term in vivo imaging of experiencedependent synaptic plasticity in adult cortex. Nature 2002;420(6917):788–794. [PubMed: 12490942]

Tsai KY, Carnevale NT, Claiborne BJ, Brown TH. Efficient mapping from neuroanatomical to electrotonic space. Networks 1994;5:21–46.

Tsai J, Grutzendler J, Duff K, Gan WB. Fibrillar amyloid deposition leads to local synaptic abnormalities and breakage of neuronal branches. Nat Neurosci 2004;7(11):1181–1183. [PubMed: 15475950]

Tsay D, Yuste R. Role of dendritic spines in action potential backpropagation: a numerical simulation study. J Neurophysiol 2002;88(5):2834–2845. [PubMed: 12424316]

Urbanc B, Cruz L, Le R, Sanders J, Ashe KH, Duff K, Stanley HE, Irizarry MC, Hyman BT. Neurotoxic effects of thioflavin S-positive amyloid deposits in transgenic mice and Alzheimer's disease. Proc Natl Acad Sci USA 2002;99(22):13990–13995. [PubMed: 12374847]

van Groen T, Kadish I, Wyss JM. Efferent connections of the anteromedial nucleus of the thalamus of the rat. Brain Res Brain Res Rev 1999;30(1):1–26. [PubMed: 10407123]

Vetter P, Roth A, Hausser M. Propagation of action potentials in dendrites depends on dendritic morphology. J Neurophysiol 2001;85(2):926–937. [PubMed: 11160523]

Walsh DM, Klyubin I, Fadeeva JV, Cullen WK, Anwyl R, Wolfe MS, Rowan MJ, Selkoe DJ. Naturally secreted oligomers of amyloid beta protein potently inhibit hippocampal long-term potentiation in vivo. Nature 2002;416(6880):535–539. [PubMed: 11932745]

Wang Q, Walsh DM, Rowan MJ, Selkoe DJ, Anwyl R. Block of long-term potentiation by naturally secreted and synthetic amyloid beta-peptide in hippocampal slices is mediated via activation of the kinases c-Jun N-terminal kinase, cyclindependent kinase 5, and p38 mitogen-activated protein kinase as well as metabotropic glutamate receptor type 5. J Neurosci 2004;24(13):3370–3378. [PubMed: 15056716]

Waters J, Schaefer A, Sakmann B. Backpropagating action potentials in neurones: measurement, mechanisms and potential functions. Prog Biophys Mol Biol 2005;87(1):145–170. [PubMed: 15471594]

Wearne SL, Rodriguez A, Ehlenberger DB, Rocher AB, Henderson SC, Hof PR. New techniques for imaging, digitization and analysis of three-dimensional neural morphology on multiple scales. Neuroscience 2005;136(3):661–680. [PubMed: 16344143]

Weaver CM, Wearne SL. Neuronal firing sensitivity to morphologic and active membrane parameters. PLoS Comput Biol 2008;4(1):e11. [PubMed: 18208320]

Wilson CJ. Cellular mechanisms controlling the strength of synapses. J Electron Microsc Tech 1988;10(3):293–313. [PubMed: 2853211]

Yadav, A.; Weaver, CM.; Gao, YZ.; Luebke, JI.; Wearne, SL. Altered mechanisms of calcium handling with age in neocortical neurons: the role of spine size and background synaptic activity. 2008 Neuroscience Meeting Planner; Society for Neuroscience, Program no. 43.20; Washington, DC. 2008a.

Yadav, A.; Weaver, CM.; Gao, YZ.; Luebke, JI.; Wearne, SL. Why are pyramidal cell firing rates increased with aging, and what can we do about it?. Proceedings of CNS Meeting; Portland. 2008b.

Yadav, A.; Weaver, CM.; Gao, YZ.; Luebke, JI.; Wearne, SL. Quantifying functional flexibility of a neuron: Effects of agerelated morphologic dystrophy in pyramidal neurons of the prefrontal cortex. 2009 Neuroscience Meeting Planner; Society for Neuroscience, Program no. 623.22; Chicago. 2009.

Ye CP, Selkoe DJ, Hartley DM. Protofibrils of amyloid betaprotein inhibit specific K^+ currents in neocortical cultures. Neurobiol Dis 2003;13(3):177–190. [PubMed: 12901832]

Yuste R, Bonhoeffer T. Morphological changes in dendritic spines associated with long-term synaptic plasticity. Annu Rev Neurosci 2001;24:1071–1089. [PubMed: 11520928]

Yuste R, Bonhoeffer T. Genesis of dendritic spines: insights from ultrastructural and imaging studies. Nat Rev Neurosci 2004;5(1):24–34. [PubMed: 14708001]

Yuste R, Majewska A, Holthoff K. From form to function: calcium compartmentalization in dendritic spines. Nat Neurosci 2000;3(7):653–659. [PubMed: 10862697]

Zador AM, Agmon-Snir H, Segev I. The morphoelectrotonic transform: a graphical approach to dendritic function. J Neurosci 1995;15:1669–1682. [PubMed: 7891127]

Zuo Y, Lin A, Chang P, Gan WB. Development of long-term dendritic spine stability in diverse regions of cerebral cortex. Neuron 2005;46(2):181–189. [PubMed: 15848798]

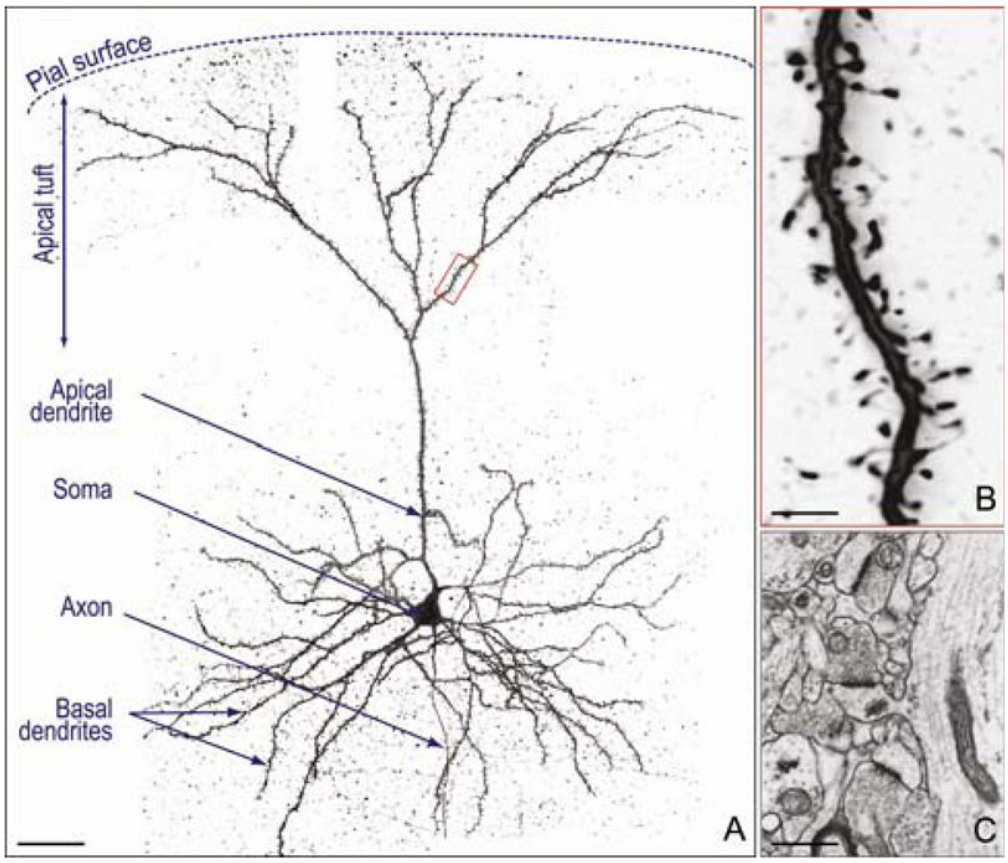

Fig. 1.

Structural properties of mouse neocortical pyramidal neurons. **a** 40 × CLSM image of a layer 3 pyramidal cell from the frontal cortex of a wild-type mouse. The neuron was filled with biocytin during patch-clamp recording and subsequently labeled with Alexastreptavidin 488. **b** 100 × CLSM image of the spiny dendrite shown within the *red box* in (**a**). **c** Electron micrograph showing the ultrastructure of a pyramidal neuron spine, with a prominent postsynaptic density and spine apparatus. Courtesy of Dr. Alan Peters. *Scale bars* **a** 40, **b** 5, **c** 0.5 μm

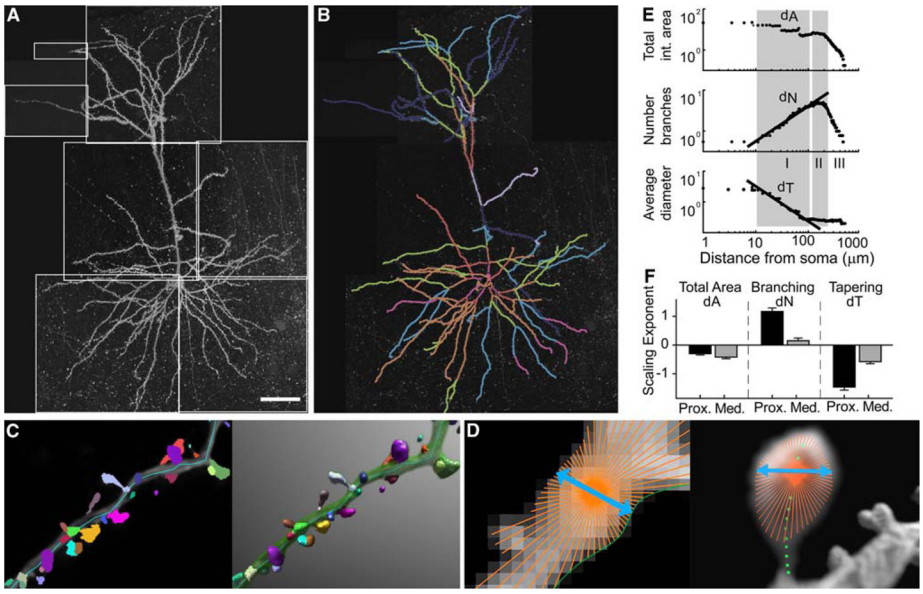

Fig. 2.

Analytical methods to quantify morphological structure. **a** *xy* projection of the montage of CLSM tiled image stacks from a wildtype mouse layer 3 frontal cortical pyramidal neuron. *Scale bar* 40 μm. **b** Tree structure from the data shown in (**a**), extracted using NeuronStudio. **c** Automatic spine detection and visualization in NeuronStudio. *Left* automatically detected spines overlaid on a maximum projection of a typical dataset; *right* the same data and spines volume-rendered in 3D. **d** *Left* 2D Rayburst sample used for diameter estimation. Rays cast using the sampling core is shown in *orange* with the one chosen as the diameter shown in *blue*. The *green line* indicates the surface detected by the Rayburst samples. *Right* spine diameter estimation using a 2D Rayburst run at the center of mass (*small green squares*) of a single layer. The *blue line* indicates the resulting width of the structure as calculated by Rayburst, and provides an approximate length of 0.7 μm. **e** Optimized fits of scaling exponents (*black fitted lines*) and optimal scaling regions (*gray shaded bands*) for the apical dendrites of a typical layer 3 pyramidal cell projecting from superior temporal cortex to area 46 (see Kabaso et al. (2009) for details). **f** Contributions of branching and tapering exponents to global mass scaling (measured by total area exponent *dA*) in spine-corrected apical dendrites of long projection neurons of young rhesus monkeys, in the proximal and medial scaling regions (*I, II* in **e**). The total branching and tapering vary across the two scaling regions, yet the total area in each region is conserved [modified from Wearne et al. (2005) and Kabaso et al. (2009)]

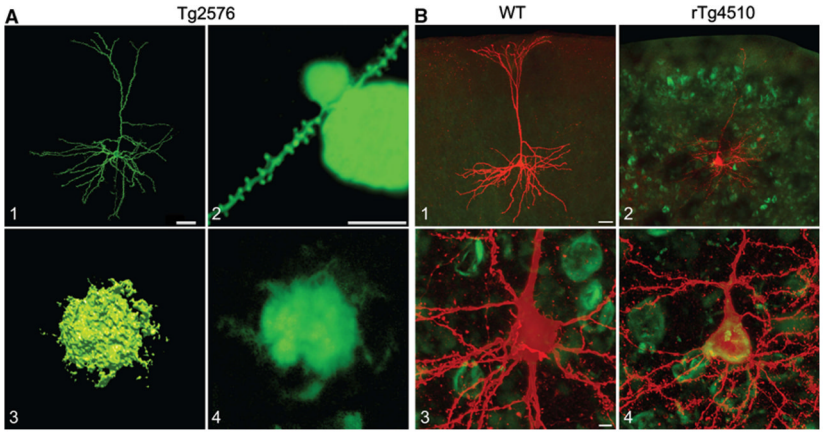

Fig. 3.

Pathological features and filled pyramidal neurons from Tg2576 and rTg4510 mice. **a** CLSM images of a Tg2576 pyramidal neuron (*1*) and a dendritic spine traversing an Aβ plaque (*2*), *3* and *4* show CLSM images of Aβ plaques. **b** CLSM images of a typical wild-type neuron (*1*) and a rTg4510 neuron pyramidal neuron containing an NFT (*2*), *3* and *4* show higher magnification views of the neuronal somata seen in *1* and *2*; **b** modified from Rocher et al. (2009). *Scale bars A1* 40 μm, *A2–4* 10 μm, *B1*, *2* 40 μm, *B3*, *4* 5 μm

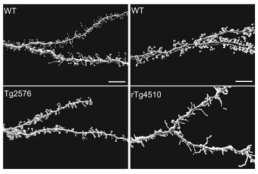

Fig. 4.

Dendritic spine loss in pyramidal neurons from Tg2576 and rTg4510 mice. CLSM images of dendritic segments with spines of neurons from wild-type (*top*) and transgenic (*bottom*) mice. *Scale bars* 10 μm [modified from Rocher et al. (2008, 2009)]

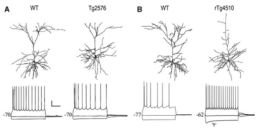

Fig. 5.

Action potential firing properties of pyramidal neurons from Tg2576 and rTg4510 mice. **a** *Top* × 40 CLSM images showing representative dendritic morphology for wild-type and Tg2576 neurons, *bottom* action potential firing properties of typical neurons. **b** *Top* 40 × CLSM images showing representative dendritic morphology for wildtype and rTg4510 neurons, *bottom* action potential firing properties of typical neurons. *Grey arrowhead* indicates depolarizing sag. *Scale bar* 20 mV, 500 ms [modified from Rocher et al. (2008, 2009)]

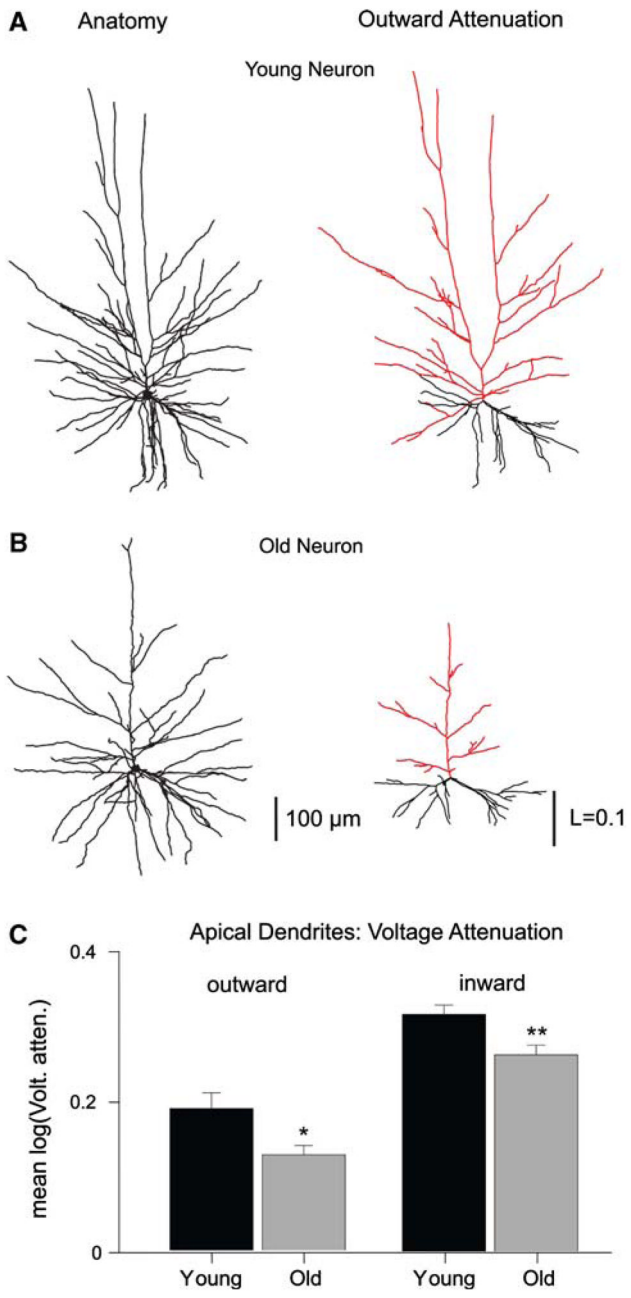

Fig. 6.

Morphological degeneration significantly affects dendritic signal propagation. **a** Anatomical reconstruction (*left*) and outward morphoelectrotonic transform (*right*) of a typical young rhesus layer 3 pyramidal cell projecting from superior temporal cortex to the PFC. Transformed apical dendrites are shown in *red*. **b** Similar to **a**, for an analogous neuron from an old rhesus monkey. **c** Effects of age-related degeneration on mean outward and outward attenuation transforms. *Histograms* shows mean ± SEM for the young (n = 24) and old (n = 19) neuron groups (*P<0.05, **P<0.01) [modified from Kabaso et al. (2009)]

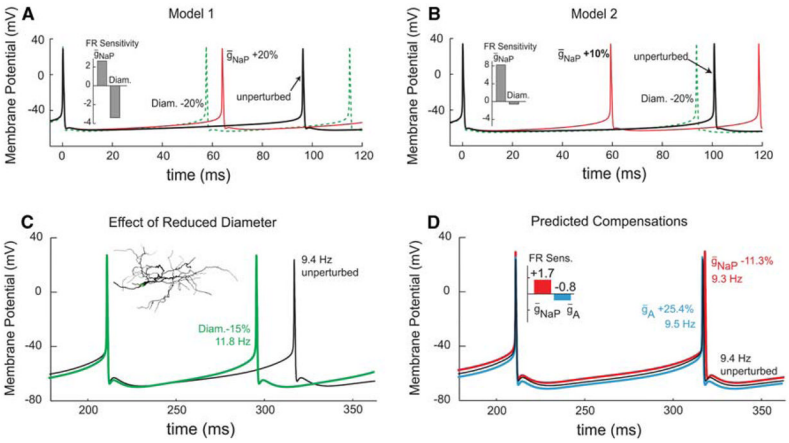

Fig. 7.

Using sensitivity analysis to predict parameter compensations that counteract the effect of morphological perturbation. **a** Comparison of morphological (*Diam.*) and conductance parameter $\bar{g}_{\mathrm{NaP}}$ perturbations of two model neurons with different combinations of membrane conductances, but similar output firing patterns. *Thick black line* shows the somatic voltage trace of the unperturbed model. *Dashed green line* shows the response to a 20% decrease in *Diam.; thin red line* shows the response to a 20% increase in $\bar{g}_{\mathrm{NaP}}$. *Inset bar plot* shows the normalized sensitivity coefficients of firing rate to *Diam.* and $\bar{g}_{\mathrm{NaP}}$: positive to $\bar{g}_{\mathrm{NaP}}$ negative and of greater magnitude to *Diam*. **b** Perturbations of the second model: analogous to those in **a**, except that the *thin red line* shows the response to a 10% increase in $\bar{g}_{\mathrm{NaP}}$ Sensitivity to *Diam.* is small and negative, while sensitivity to $\bar{g}_{\mathrm{NaP}}$ is large and positive. **c** In a model of goldfish precerebellar neurons (morphology shown *inset*), a 15% reduction in *Diam.* increased firing rate by 20.3% relative to the unperturbed value. **d** The compensatory perturbations of two different conductance parameters ($\bar{g}_{\mathrm{NaP}}$ in *red*, shifted vertically up; $\bar{g}_{\mathrm{A}}$ in *blue*, shifted down) were predicted from their firing rate sensitivities (*inset bar plots*). The *blue* and *red* compensated traces overlie the unperturbed (*black*) trace very closely, demonstrating excellent compensation [modified from Weaver and Wearne (2008)]